To the Graduate Council:

I am submitting herewith a thesis written by Matthew Wayne Fuller entitled “High Permittivity and High Permeability of Nanoparticles in Conducting Polymer Films.” I have examined the final electronic copy of this thesis for form and content and recommend that it be accepted in partial fulfillment of the requirements for the degree of Master of Science, with a major in Material Science Engineering

Dr. Bin Hu, Major Professor

We have read this thesis
and recommend its acceptance:

Roberto Benson

Kevin Kit

Accepted for the Council:

Carolyn R. Hodges, Vice Provost and
Dean of the Graduate School

(Original signatures are on file with official student records.)

High Permittivity and High Permeability of Nanoparticles in Conducting Polymer Films

A Thesis
Presented for the
Master of Science
Degree
The University of Tennessee, Knoxville

Matthew Wayne Fuller
August 2009

ACKNOWLEDGEMENTS

I would like to ultimately thank our Lord Jesus Christ for giving me the opportunity to perform this research and to earn the degree for which this thesis has been written in partial fulfillment. I would also like to thank my family; Cheris, Brandon and Rylan, for the sacrifices they had to make for the time put into this research and lab work and the writing of the thesis. I would also like to thank Dr. Benson for the opportunity to be admitted into the Master's program in Material Science. I would like to also thank Dr. Hu for the guidance in the research and testing of the samples and Dr. Kit for information from various classes. Finally, I would like to thank everyone in Dr. Hu's group, especially Yan Liang and Huidong Zang, Tommy Washington and Tiffany Flick for their help in preparation and testing samples.

ABSTRACT

The purpose of this study is to synthesize a new material out of conducting polymers and magnetic nanoparticles that has high electric permittivity and high magnetic permeability. There is a strong desire in electronics for lighter, faster, cheaper and more bandwidth providing materials. There is also an interest with the military for materials that are light weight, have high electric permittivity and high magnetic permeability. A way to synthesize a material that meets those criteria is to use conducting polymers for their high permittivity properties and to disperse magnetic particles in the polymer for their high permeability properties. The synthesized material can be tuned to gain the desired measure of both permittivity and permeability and to achieve a low dielectric loss. There is also a need for electromagnetic shielding and absorption properties. Polymers that conduct electricity, so called synthetic metals such as polypyrrol and poly-p-phenylene, coupled with magnetic nanoparticles (iron, cobalt or nickel) can positively benefit the electronics industry in the previously mentioned properties. In the present thesis, Polymer A and Polymer B were blended with nanoparticles in various solvents and differing weight fractions of nanoparticles. The samples were tested on various spectrometers to find the reaction to the electromagnetic spectrum. The nanoparticle size and morphology were determined by using a Scanning Electron Microscope (SEM). The values for permittivity and permeability were determined for various concentrations of carbon coated

nanoparticles by using various instruments. The results yielded high permittivity and moderate permeability.

TABLE OF CONTENTS

Chapter Page

LIST OF FIGURES

Figure Page

LIST OF TABLES

CHAPTER 1

Introduction to Conducting Polymers and Nanoparticles

1.1 Polymers

Polymer science was started in industrial laboratories due to the need to manufacture and to understand new materials (rubbers, plastics, adhesives, fibers, and paints). Only much later did polymer science come to academia. Polymer science tends to be more interdisciplinary than most sciences combining chemistry, materials and other fields.[1]

Polymers are basically long chains of molecules that have high molecular weight, often measured in hundreds of thousands (grams per Mol). Polymers started out as study of natural products (cotton, starch, cellulose and wool) and the twentieth century were extended to synthetic polymers were made. Some of the original synthetic polymers were Bakelite and nylon.[1]

Some aspects of polymers include their molecular weight and molecular weight distribution and how their atoms are organized within the chain. Many polymers crystallize and the configuration of the crystalline material can depend on the conditions the polymer was crystallized with. Some polymers do not crystallize and are called amorphous polymers. Thermal behavior of the polymer depends on its molecular weight and molecular structure. One of the important thermal properties is the glass transition temperature, the temperature where the

polymer goes from a glassy state to a rubbery state. Other molecular structure dependent properties includes; modulus, stress relaxation and elongation to break.[1]

1.2 Conducting Polymers

Conducting polymers became well known in 2000 when Alan J. Heeger, Alan G. Mac-Diarmid and Hideki Shirakawa were awarded the Nobel Prize in Chemistry for the discovery and development of conducting Polymers.[2] Conducting polymers carry a current in the same manner as metals; they give up a free electron to create current. This phenomenon is observed in conjugated polymers. See Figure 1 in the Appendix (all tables and figures are in the Appendix) for chemical formulas of some conducting polymers. The miniaturization of electronics and need for high frequency filters has made a need for a new type of materials with high permittivity, high permeability and low dielectric loss.

The structural requirement for a conducting polymer is a π-conjugated electron system constituting the polymer backbone, but conducting polymers are also possible when the π-conjugated electron system is present in side chains. The mechanism for electrical conduction in polymers can be viewed in Figure 2. Strong interactions with the π-conjugated electron indicate a high delocalized structure and large valence bandwidth. Ionization potential (IP) must be small for good conductivity. IP is the energy needed to remove an electron from an atom.

Electron Affinity (EA) shows the ease of addition of an electron to the polymer. Band gap (E_g) is a representation of the optical-absorption threshold. Bandwidth (BW) represents the carrier mobility and the higher this value is the better for the polymer to conduct. [1,3,4]

The largest and most immediate potential application for conducting polymers is lightweight rechargeable batteries for portable devices (e.g. tools) and vehicles. Conducting polymers would serve both current carrying and ion-conduction functions by replacing traditional electrode and electrolyte substances. The other application area for conducting polymers is their use to build circuitry elements, both passive (conducting circuits) and active.[1]

1.3 Nanoparticles

Nanoparticles have become an interesting topic among the various science fields due to the unique properties (listed below) of the material at very small particle size. There is no strict dividing line between nanoparticles and non-nanoparticles. The size at which materials display different properties to the bulk material is material dependent and can certainly be claimed for many materials much larger in size than 100 nm.[5] An example of how a material behaves differently in the bulk form than the nano form is Iron. In the bulk form the element is stable, but in the nano form it is highly flammable in an oxygen environment. Nanoparticles offer the benefit of needed properties that can be easily added to another bulk material. The following properties are entirely

dependent on the fact that at the nano-scale, the physics of nanoparticles mean that their properties are different from the properties of the bulk material: micro-mechanical, elasticity, strength and stability properties.

1.4 Composite Materials

Composite materials have been around for hundreds of years so the idea is not new to add two or more materials that are different to synthesize a material with properties vastly different than the individual constituents. One composite family is to combine the electrical and light-weight properties of polymers with magnetic materials to fine tune the composite for distinct applications.

Polymer composites used in Construction (civil engineering) and building industries account for approximately 30% of all polymers produced each year. Polymers offer many advantages over conventional metals including lightweight, resistance to corrosion and ease of processing. They can be combined with fibers to form composites which have enhanced properties, enabling them to be used as structural members and units. Polymer composites can be used in many different forms ranging from structural composites in the construction industry to the high technology composites of the aerospace and space satellite industries.[5]

New materials can be found by combining conducting polymers with magnetic particles in a new synthesized material. Polymer processing is much easier (extrusion, injection molding, etc.) than forming metal for electronic

applications. The use of conducting polymers would make certain types of applications more practical and economical.

1.5 Physics of Dipoles

Materials that normally do not conduct electricity and can store an electrical charge are called dielectrics. Polymer engineers are concerned with understanding the role of long chains of polymers in differing applications, such as heat resistant dielectrics to self repairing plastics. Organic polymers (ex. Poly Amides and conjugated dienes) are stable materials at high temperatures (some up to 500 ^{O}F)[6] and can withstand radiation (30-100 Mega Gray (MGy) units).[7] These properties make the polymers desirable to many different applications such as in nuclear power plants and, in the space environment, on satellites or space vehicles. Polymer materials have the ability to store electrical charges. [8]

Any neutral molecule is a system of electric charges distributed in space. Positive charges are concentrated in the nucleus and negative charges are spread out in the electron cloud and can be manipulated by electric fields.[9] An electric dipole is a pair of equal and opposite charges in close proximity to each other. Figure 3 shows a schematic for the dipole interaction. A dipole moment is $\mu = Q * d$, where "*Q*" is a charge and "*d"* is the distance between the two charges, μ is a vector quantity.[3]

Figure 4 Shows the interaction between the polymer chain and the magnetic nanoparticle. "μ" is the dipole moment as defined above and "P" is the

potential due to the dipole. There are two interactions between the polymer chain and the magnetic nanoparticle: one interaction is electrical with the magnetic nanoparticle aiding in the conductivity of the polymer (the nanoparticle is considered a dopant); and the second interaction is a magnetic influence on the polymer molecules (specifically the electrons with the dipoles) by the magnetic nanoparticle.

Particle-polymer bonding and enhanced interfacial zone (surface area between polymer and nanoparticle) plays a very important role in determining the dielectric behavior of nanocomposites.[10] The free volume in such interaction zones is altered by the introduction of nanoparticles. Since these interaction zones are likely to overlap at relatively low volume fractions in nanocomposites, a small amount of nanoparticles has been found to impact the electrical behavior. There is literature (Chapter 4.8) that emphasizes the interaction zone around the particles is a quasi-conductive region which partially overlaps in the nanocomposites. These overlapped interface regions allow charge dissipation. The charge dissipation could be expected to improve the dielectric breakdown strength and voltage endurance characteristics.[10] The electrical effect of the nanoparticle on the polymer is one of a donating electron, if the nanoparticle is coated with a conducting material (ex. Carbon with a free electron).

Due to the size of the nanoparticle (approximately 50 nm) each nanoparticle becomes a single magnetic domain and shows superparamagnetic

behavior when the temperature is above the so-called blocking temperature. Such individual nanoparticles have a large constant magnetic moment and behave like a giant paramagnetic atom with a fast response to applied magnetic fields with negligible residual magnetism and coercivity (the field required to bring the magnetization to zero).[11]

The different magnetic effects occurring in the polymer and magnetic nanoparticles is figuratively laid out in Figure 5.[11] Block (A) material represents a ferromagnet material. The arrows represent magnetic lines of flux. Block (B) material is an antiferromagnet with weak ferromagnetism. Block (B) represents the polymer matrix with the hysteresis curve located in Block (E). Block (C) is a representation of the superparamagnet nanoparticles and the associated hysteresis curve. Block (D) is the most interesting block representing the polymer/magnetic nanoparticle composite. This material has combined effects of the polymer and the magnetic nanoparticles. The interaction can clearly be seen between the ferromagnetic material and the antiferromagnet material in the hysteresis curve in Block (D).[11] Block (F) is the hysteresis curve for the pure ferromagnet material (for reference). The hysteresis curve of the composite material is a trade-off between the pure ferromagnetic material (Block (F) and the antiferromagnet material (Block (B). This curve can be tailored to the specific application of the composite by adding or subtracting nanoparticles to the polymer. This composite hysteresis curve is due to the dipole-dipole interaction

between the magnetic nanoparticle and the electrons in the polymer chain.[11] The Results Chapter will reference these phenomena in the various tests that were performed on the polymer/nanoparticle composite.

The above mentioned affects should be progressively greater for a larger percent on nanoparticles added to the polymer composite.

1.6 Desired Research

Research is needed to find suitable composites that have properties of conducting polymers and of magnetic nanoparticles. The composite can be made into thin films that can be used for a variety of applications. Some uses for thin film composites are optical coatings for use in aircraft displays, helmet visor coatings and stealth applications (microwave absorption).

The properties needed from conducting polymers are electronic and optoelectronic properties. Electronic properties include conduction and optoelectronic properties include transmission/absorbance. Conducting polymers have weak ferromagnetic properties. An example of a device that uses conducting polymers is the field effect transistors.

The magnetic (ferromagnetic) properties are needed from the nanoparticles. Some magnetic nanoparticles are iron, cobalt and nickel. All three of these nanoparticles should produce a strong dipole moment. The nanoparticles have some intrinsic electronic properties (such as the Carbon coating conducting electricity), but would need another material to exploit more

favorable electrical and optical properties. Some examples of devices using magnetic properties from nanoparticles are light emitting diodes and solar cells.

Permittivity, ε is a measure of the extent to which it concentrates electrostatic lines of flux. It is the ratio of the amount of stored electrical energy when a potential is applied, relative to the permittivity of a vacuum.[3] Solving the following equation will give permittivity where C is capacitance, ϵ is the permittivity and A is the area.

$$C = \frac{\epsilon A}{d} \quad (3)$$

Magnetic permeability, μ is the product of the permeability of free space (vacuum) or absolute permeability (μ_0) and relative permeability of the medium (μ_r). Permeability is the relative increase or decrease in the magnetic field inside a material compared with the magnetic field in which the material is located. In empty space, the magnetic permeability is 1, because there is no matter to modify the field. Materials may be classified by the value of their magnetic permeability.[3] Solving the following equation will give permeability where n = index of refraction, μ = permeability and ϵ = permittivity.

$$n = (\mu * \epsilon)^{1/2} \quad (3)$$

Index of Refraction (symbol n) is the ratio of the speed of light in a vacuum to the speed of light through a medium.[3] Also, commonly called “Refractive Index”. The equation for index of refraction is

$$V = {}^{c}/_{n}$$

where *v* is the speed of light in the medium and *c* is the speed of light in free space.[8]

1.7 Anticipated Results

This research should yield a composite material with increasing electric permittivity and magnetic permeability in direct relationship with increasing magnetic nanoparticles added to the composite. Although there is currently no way to measure the microwave absorptivity where the research was performed, the absorptivity should also increase with more nanoparticles added to the composite. Note: microwave absorptivity is an item of interest and research in the literature and will be discussed in Chapter four.

1.8 Research Methodology

The research was conducted in three parts:

First, the literature was consulted and there was found to be some work similar in nature to the research to be studied. The literature review is presented in Chapter 2 of this thesis. The reported studies dealt primarily with using

conducting polymers and some form of Iron Nanoparticles. In this thesis a composition of conducting polymers were used and nanoparticles were synthesized. The nanoparticles should prove easier to use in the manufacturing of the thin films due to the explosive nature of the iron nanoparticles.

Second, the samples were manufactured so they could be tested. In the manufacturing process the two polymers were either bought in a suitable solvent (POLYMER A) or one was added to the polymer (Polymer B). Nanoparticles were added to the samples in varying amounts by total weight of the polymer/nanoparticle composite. Samples were then spun cast.

Third, the samples were tested on various instruments (FTIR, SEM, UV-Vis, Luminescence, ellipsometer, etc.) and the data was recorded. The information was placed in a usable format (either graph or table) and reported in Chapter 5 of this thesis.

CHAPTER 2

Literature Review

2.1 Chapter Overview

There were several papers with similar topics as this thesis. Most of the papers discuss experiments with some form of iron oxide and Polyaniline (PANI). The problem with iron oxides is when they are in the nano form, they are combustible in an oxygen environment; therefore, special handling becomes necessary when it is used in manufacturing samples. In this thesis, nanoparticles were used which have similar magnetic properties without the combustibility of the iron oxides. The nanoparticles that were used were covered with carbon to aid in stability, but for the experimentation, the carbon actually improves the conductance of the polymers.

2.2 Dielectric, Magnetic and Microwave Absorbing Properties of Iron Particles Dispersed In Rubber Matrix in Gigahertz Frequencies

Several papers were written on dielectric, magnetic, and microwave absorbing properties with polymers and some form of iron oxide. One paper used a rubber matrix and dispersed milled iron flakes into the polymer.[14] The focus of the research was to develop high frequency electromagnetic properties (in the gigahertz frequencies) for thin microwave absorbers for use as noise absorbers

and wave impedance matching. Low eddy current loss was attributed to the milling of the iron particle. The study used the high magnetic permeability and dielectric constant for favorable wave impedance matching. The results were permeability and permittivity both increased at a greater value with iron flakes verses iron spheres due to eddy current losses in the spheres.[14]

2.3 High Frequency Properties of Polymer Composites Consisting of Aligned Fe Flakes

Zhang et al. has published a paper that used iron nano flakes and aligned them in one direction using a manufacturing technique (polymer extrusion). By aligning the flakes, they effectively increased the magnetization and lowered the eddy current loss effect (due to the large aspect ratio).[15] The author mixed the flakes with either polystyrene (PS) or polymethylmethacrylate (PMMA) in weight fractions from 15% to 50%. The flakes were coated with a thin layer of silica to eliminate the eddy current. The mixture of either PS or PMMA was heated to 200 ^{0}C and extruded to align the flakes preferentially. Several instruments were used to measure the real and complex permittivity and permeability spectra. The index of refraction was also computed in this study for the samples.[15] The reported indexes of refraction for their samples are: 5.5 for 15% nanoparticles; 9.5 for 25% nanoparticles; and 26.5 for 50% nanoparticles. The graph of permittivity for this literature combined with this thesis work is in Figure 27. [15] The results will be discussed in Chapter 5.

2.4 Polyaniline/magnetic ferrite nanocomposites obtained by in situ polymerization

PANI was synthesized with $Zn_{0.6}Cu_{0.4}Cr_{0.5}Fe_{1.5}O_4$ magnetic nanoparticles with varying weight fractions. The weight fractions used were 10% and 20% of magnetic nanoparticles.[16] The ferromagnetic behaviors of nanocomposites were investigated as a function of the content of $Zn_{0.6}Cu_{0.4}Cr_{0.5}Fe_{1.5}O_4$ particles. Recently, magnetic ferrites have displayed a promising application in microwave absorption due to the electromagnetic loss derived from their complex permittivity and permeability. It is known that the conducting polymers can effectively shield against an electric field, but only magnetic material can shield waves from a magnetic field, especially at low frequencies.[16] Thus, through fabrication of the conducting polyaniline–magnetic ferrite composites used as EMI shielding materials, good shielding effectiveness can be achieved for various electromagnetic sources.[16] Based on these factors, there is a motivation to synthesize conductive and magnetic composites suitable for shielding applications.[10] This research performed some of the same test analyses that was performed in this thesis, which are listed below and will be discussed in Chapter five.

UV-Vis wavelength analysis was performed on the PANI and $Zn_{0.6}Cu_{0.4}Cr_{0.5}Fe_{1.5}O_4$ magnetic nanoparticles. The data is in Figure 7.

Infrared Spectra were collected for the samples of PANI and $Zn_{0.6}Cu_{0.4}Cr_{0.5}Fe_{1.5}O_4$ magnetic nanoparticles. A composite of the infrared spectra is presented in Figure 8. Note: The data for FTIR from this study is presented in transmittance, which is the opposite of absorbance presented in this thesis.

The SEM was used to determine the morphology of the samples. The SEM pictures are located in Figure 9.

In summary: Magnetic parameters such as saturation magnetization and coercivity of the nanocomposites directly rely on percent weight of the particle.[16]

2.5 Surface properties of polyaniline/nano-TiO2 composites

Polyaniline/nano-TiO2 composite was prepared by polyaniline for the surface modification of nano-TiO2 particles and was characterized via FTIR spectra, UV-Vis near infrared spectrometer.[17] The results of spectroanalysis illustrate that polyaniline and nano-TiO_2 particles are not simply blended. There is a strong interaction between polyaniline macromolecule and nano-TiO2 particles. Synthesized polyaniline was deposited on the surface of nano-TiO2 particles, forming a core-shell structure. The dimension of polyaniline/nano-TiO2 composite particles is in the range 25–40 nm.[17]

UV-Vis wavelength analysis was performed on the PANI and TiO_2 nanoparticles. The data is in Figure 10

Infrared Spectra was performed on the samples of PANI and TiO_2 nanoparticles. Note: The data for FTIR from this literature[17] is presented in transmittance, which is the opposite of absorbance presented in this thesis. The FTIR data is located in Figure 11.

In Summary: Fourier-transform infrared spectra and UV-Vis-NIR spectra indicate that polyaniline and nano-TiO_2 particles are not simply blended. A strong interaction exists at the interface of polyaniline macromolecule and nano-TiO2 particles.[17]

2.6 Polymer Nano-Layer Coatings for Optical Application

A deposition process was used to control nano meter thin films in multiple layers to achieve specific optical properties. The multilayered coatings can be used in aircraft canopies, pilot visors and display panels.[18] The purpose is to control absorbance/transmittance properties. Polymers are used due to their ease in processability and the benefit of weight savings for the aerospace industry. The authors used a new technique for the deposition process; plasma enhanced chemical vapor. The new process can also polymerize organic monomer compounds that previously could not be used.[18] Follow on research could be used for this thesis for the same purpose as this literature due to the same processes being used and the same material properties being sought after.

2.7 Magnetic and Microwave Absorbing Properties of Polyaniline/γ-Fe_2O_3 Nanocomposite

Microwave absorption is important in electromagnetic shielding and stealth technology for vehicles.[19] This investigation used PANI in testing for microwave absorption. The composite consisted of PANI and Fe_2O_3 rod like shapes of magnetic nanoparticles. The nanoparticles were synthesized by a chemical sol-gel route. Then the mixture was dried. They also used PANI in emraldine Salt and used in-situ polymerization and then dried the polymer/nanoparticles. The absorbance properties of the composite were tested by dispersing the sample in a wax coating and deposited on an aluminum substrate.[19] The samples were analyzed using a vector network analyzer. The results were microwave absorbing properties were high for the samples prepared with up to 20% (by weight) nanoparticles. In the samples with greater than 20% (by weight) nanoparticles the microwave absorption decreased. The magnetic loss tan and dielectric loss tan also decreased above 20% nanoparticles (by weight).[19] In this thesis there was no capability to measure the microwave absorbing properties of the samples. Further research would need to be done on the microwave absorbing properties of Polymer A with magnetic nanoparticles and Polymer B with magnetic nanoparticles.

2.8 Magnetic Nanoparticles: Synthesis, Protection, Functionalization, and Application

An-Hui et al. focused on the magnetic properties of nanoparticle systems. They used various polymerization techniques to combine the nanoparticles with the polymer (ex. co-precipitation, thermal decomposition and/or reduction, micelle synthesis, and hydrothermal synthesis). One of their interests was protecting the magnetic nanoparticle from oxidation and chemical attack (corrosion) that would leave the nanoparticle with degraded or low magnetism.[10,20] The nanoparticles are unstable over long periods of time in pure form. The particles tend to aggregate to reduce the energy associated with their high surface area to volume ratio.[20] As previously discussed (iron nanoparticles combustibility) most pure-metal nanoparticles are chemically highly active if not treated resulting generally in loss of magnetism and dispersibility. The techniques the author used to alleviate the volatility of the nanoparticles was to coat them in a polymer matrix, coat them in silica, or cover them with carbon. [10,20]

Magnetic interparticle interactions between the polymer and the nanoparticle are; dipole–dipole interactions, direct exchange interactions for touching particles and superexchange interactions for metal particles in an insulating matrix. Dipolar interactions are almost always present in a magnetic particle system and are the most relevant interactions. They are anisotropic. [10,20]

Surface Effects of the nanoparticles increase inversely with nanoparticle size (the percentage of surface of the nanoparticles increases due to the particle becoming smaller). As the size of the nanoparticle decreases the percentage of surface atoms increases. This implies that surface and interface effects become more important. A majority of electron spins are surface spins, which are an important contribution to the magnetization. The authors reported for small metallic nanoparticles (Cobalt) there was an enhancement of the magnetic moment with a "magnetically dead layer" (using carbon to coat the nanoparticle).[20] The coupling of the ferromagnetic particles with an antiferromagnet matrix is a source of a large additional anisotropy (large magnetic flux).[20] Furthermore, the exchange coupling can supply the extra anisotropy which is needed for magnetization stabilization, thus generating magnetically stable particles.[20] mechanism. The synthesis of dispersible, carbon-coated nanoparticles in isolated form is currently one of the challenges in this field.

2.9 Synthesis and Electro-magnetic Properties of Polyaniline-barium Ferrite Nanocomposite

Yuan-xun Li et al. Discuss adding magnetic properties with the electric properties in a composite. PANI was used with barium ferrite ($BaFe_{12}O_{19}$) to gain the desired properties of an electromagnetic inference (EMI) shielding material and broadband microwave adsorbing material.[21] The barium ferrite has the material

properties to absorb the microwave radiation. Interactions between the polymer and the barium ferrite can be seen with the hysteresis curve in Figure 12. Curve (a) is pure barium ferrite which displays a typical hysteresis curve for a ferromagnetic material. Curve (b) shows a similar curve but is not the characteristic ferromagnetic curve.[21] The composite exhibited a decrease in the hysteresis curve (as compared to pure ferromagnetic material) due to the existence of PANI (low magnetism) and the interaction between magnetic nanoparticles and nonmagnetic medium by the dipole-dipole interactions, which contribute to magnetic anisotropy and consequently change the magnetic properties of the nanoparticles. For the PANI-barium ferrite composite system, with the decrease of surface anisotropy upon coating and the increase of interparticle distances which will lead to weakened interparticle interaction, the decrease in coercivity and magnetization is expected in the composite material as compared to the pure ferromagnetic material.[21] There was a substantial increase in magnetism in the composite over pure PANI.

2.10 Complex Permeability and Permittivity and Microwave Absorption Property of Barium Ferrite/EPDM Rubber Radar Absorbing Materials in 2-18GHz

Yongbao et al. presents a paper that tests the difference in permittivity and permeability in a composite of rubber and barium ferrite (RADAR absorbing Material (RAM)) for microwave absorption. The volume fractions and thickness

of the RAM were varied and studied.[22] The real permittivity spectra of the radar absorbing materials increase as the ferrite volume fraction increases. The imaginary permeability spectra increase as the ferrite volume fraction increases. The reflectivity of the radar absorbing materials is proportional to the thickness and barium ferrite volume fraction when the volume fraction and the thickness are 10% and 1.0mm.[22] Figure 13 is a graph of the complex permeability with volume fractions from 10% up to 50% in increments of ten percent. The permeability shows a steady increase for an increase in magnetic nanoparticles. The conclusions of the graph can be found in Chapter 5.9.

CHAPTER 3

Experimental Preparation

3.1 Materials Used

Several samples were made using both Polymer A and Polymer B. Polymer A came from the manufacturer (Sigma-Aldrich) in a xylene emraldine salt. Polymer B was in the form of a powder (pure polymer) from the manufacturer (Sigma-Aldrich USA). The composite samples were prepared with magnetic-carbon-coated nanoparticles from Sigma Aldrich USA. The manufacturer listed the nanoparticle size at 50 nm. The polymers were added to a solvent and then the nanoparticles were added to the solution and went into a suspension. Polymer A was already in a suitable solvent (xylene) in a 2-3% by weight concentration. Polymer B was mixed with chloroform.

The reason the nanoparticles were chosen, instead of iron nanoparticles, is due to the explosive nature of iron nanoparticles in an oxygen environment. The nanoparticles needed no special handling compared to the use of the iron nanoparticles.

3.2 Sample Substrate and Other Glassware Preparation

All glassware used in the preparation of samples was cleaned in the following manner; the articles were placed in a glass container with industrial cleaner

(Fisher Brand Versa Clean USA) and placed in a sonic mixer for at least thirty minutes. Then, the articles were triple washed with de-ionized water, triple washed with acetone and triple washed with chloroform (reagent grade). Finally, the articles were placed inside a Fisher Vacuum Oven (Figure 14) for a half hour to dry.

3.3 Synthesis of Polymer A Composite with Nanoparticles

The Polymer A that was purchased for the synthesis came as a green liquid in an emraldine salt (2-3% weight) dispersed in xylene. The polymer and carbon coated nanoparticles were purchased from Sigma-Aldrich Chemical Company. The nanoparticles were added by the following weight fractions: 5%, 10% and 15%. The composite mixture was placed into a sonic mixer for thirty minutes. After the thirty minutes the mixture was checked and the particles were observed to be suspended in solution (no particles settling to the bottom of the glass container and no particles coating the side of the glass container). Eventually the particles will settle out of solution, but that takes several hours, which is more than enough time to spin cast the samples. (The spin cast process is addressed later in this thesis.)

3.4 Synthesis of Polymer B Composite with Nanoparticles

The Polymer B that was purchased for the synthesis came as an orange-red powder. The nanoparticles were added by the following weight fractions; 5%,

10% and 15%. The polymer and the nanoparticles were added to a solvent (Chloroform). The composite mixture was placed into a sonic mixer for thirty minutes. After the thirty minutes, the mixture was checked and the particles were observed to be suspended in solution (eventually, the particles will settle out of solution, but that takes several hours, which is more than enough time to spin cast the samples).

3.5 Preparation of Glass Substrate

The glass substrates (half coated with Iridium Titanium Oxide from the manufacturer) were made by the following process: Using a volt meter to correctly identify the ITO side, the glass substrates were placed inside a jig for ease of soldiering. It was possible to prepare four glass substrates at a time with the jig. Once all four substrates were in the jig, the wires were prepared by cutting them off the spool and then rolling under a piece of glass to straighten. Standard copper was used for the wire leads. Then the wires were placed on the jig with tweezers. The wires were soldered in place using a glass dropper and microcircuit brand solder (Silver Type “L”). Once all of the wires were placed and soldered (16 total wires), the jig was placed on a hotplate for fifteen minutes to cure the solder. Once the solder was cured, the substrates were cleaned in the same process outlined in Chapter 3.1.

3.6 Spin Casting Solutions onto Glass Substrate

The substrates were placed inside the spin cast machine, Figure 15, along with the polymer and polymer/nanoparticle samples. The substrates were placed on the vacuum spinner head and the polymer and polymer/nanoparticles were individually dropped onto the substrate and then spun at a RPM for a specific time. The samples were spun to facilitate a uniform thin film surface for the aluminum to adhere by evaporation (electrode). Some polymer solutions were diluted with additional solvent and spinning was delayed a few minutes to allow evaporation. There were three variables in spin casting samples. The variables are: RPM of the spinner, spin time and solvent evaporation time. See Table 1 for sample RPM, spin times and/or evaporation time. These variables were fine tuned for each sample set taking into consideration solution viscosity.

Note: Two sets of samples were made. One set with ITO on the substrate plus electrodes and one set without ITO or electrodes.

3.7 Aluminum Electrode Evaporation

All of the samples were placed in the aluminum evaporator, Figure 16, to install aluminum electrodes on the films/samples. The whole process takes about four hours and requires a high vacuum for the process to deposit aluminum on the samples. Refer to Figure 17 for pictures of samples with electrodes vacuum deposited over the thin film. The process was started by releasing the vacuum.

(The machine is stored in a vacuum state to keep contaminates out of the system.) The samples were loaded in the test chamber and the solid aluminum ingot was placed on the crucible. The test chamber was closed (the test chamber is the steel barrel on top of the machine in Figure 16). Next the system was purged with nitrogen gas. After the system was purged the nitrogen gas was turned off. The vacuum pump was turned on until the pressure was 2.0 E-2 Torr. Once the pressure reached 2.0 E-2 Torr the turbo pump was turned on until the pressure was brought down to 3-5 E-6 Torr. Next the deposition module was turned on along with the heat to the aluminum ingot. After the aluminum was in a molten state the shutter was opened which allowed the aluminum vapor to deposit on the samples. The amount of aluminum deposited on the samples was controlled with the deposition module. The thickness of aluminum on the samples was in a range of 0.5-0.8 **Å** (or 0.05-0.08 nm). Once the desired thickness was achieved, the modules were turned off. After twenty minutes the test chamber cools down to room temperature and the system was purged with nitrogen. Then the samples were retrieved.

3.8 Samples Ready for Testing

Figure 17 shows the samples as they are ready for testing. The glass substrate was on the bottom and it comes from the manufacturer with the ITO already on half of the substrate. See Figure 18 for a schematic of the glass substrates with electrodes. The next layer was the polymer nanoparticle composite that had

been spun cast. The top layer was the aluminum deposition layer. The copper wires have been omitted for ease of visualization.

Samples were also prepared for various testing without electrodes (UV-Vis, FTIR, etc.). Figure 19 shows the samples without electrodes.

Samples were also made on a silica substrate for the index of refraction test. These samples can be seen in Figure 20.

CHAPTER 4

Testing

4.1 Instrumentation

Several instruments were used in preparation of samples and measuring the samples. The Cook Vacuum aluminum deposition machine, Figure 16, was used to deposit aluminum electrodes on the samples. The vacuum oven, Figure 14, was used to ensure there was no solvent left in cleaning glassware and substrate and to ensure no moisture was present in the samples designated for FTIR studies. A locally fabricated spin caster was used in sample preparation, Figure 15. The Bio Rad FTS 6000e Fourier Transform Infrared (FTIR) Spectrometer was used to gain spectral absorbance information on the samples, Figure 21. A Lambda 35 UV-Vis spectrometer was used to analyze the samples (Figure 22) along with a Fluorolog photoluminescence instrument made by Jobin Yvon Horiba (Figure 23). A Gemini Leo 1525 Scanning Electron Microscope (SEM) was used to study the morphology of film samples (Figure 24). The Agilent E4980A Precision LCR Meter was used to measure the capacitance of the samples. The Gaertner Ellipsometer was used to determine the film thickness and the index of refraction (Figure 25).

4.2 Fourier Transform Infrared (FTIR) Spectrometer

The samples were prepared for the FTIR by using two techniques: film deposition and KBr pellets.

Liquid samples of Polymer A were prepared by use of a KBr crystal. The Polymer A polymer solution was dropped onto the KBr crystal and the solvent (Xylene) was allowed to evaporate leaving the Polymer A film and nanoparticles deposited directly on the crystal. The crystal/sample was dried in the vacuum oven for 24 hours. The crystal/Polymer A film was placed inside the test Chamber. Again, due to the chemical nature of KBr (KBr does not radiate IR radiation) only the polymer and nanoparticles were analyzed.

Powder samples of Polymer B were analyzed by using potassium bromide (KBr) pellet. The samples must be dried in the vacuum oven for 24 hours. Then samples were added to KBr and then pressed into pellet form using a steel press. The pellet was inserted into the FTIR instrument and due to the lack of radiation by KBr, only the polymer and nanoparticles were analyzed by the FTIR instrument.

Absorbance from the FTIR is calculated by the FTIR instrument by the motion of the mirrors inside the instrument. The FTIR detector measures intensities only (wavelength is not a factor). If there is no change in the two paths inside the instrument then there is no interference, but if there is a

difference in the path lengths then there is constructive interference and the peaks are registered in the software.[12]

4.3 UV-Vis Spectrometer

A Lambda 35 Ultra-violet/Visible spectrometer was used to gather UV-Vis data on the spin cast samples without electrodes, Figure 22. The scan speed was set at 240.0 nm/min. First, there are two transmission holes, one for samples and one for blank substrate. The instrument needs a warm up period of approximately fifteen minutes after it is turned on. Second, the instrument is calibrated with two blank glass substrates. After calibration the instrument can run on the samples needed to be analyzed without a recalibration.

Absorbance in the UV-Vis region measures transitions from the ground state to the excited state.[13] The Instrument measures the intensity of light passing through a sample (I), and compares it to the intensity of light before it passes through the sample (I_o). The ratio I / I_o is called the *transmittance*, and is usually expressed as a percentage (%T). The absorbance A, is based on the following equation:

$$A = -\log (\%T / 100\%).^{(13)}$$

4.4 Photoluminescence

The samples were run on the Fluorolog Photoluminescence instrument manufactured by Jobin Yvon Horiba, Figure 23. Photoluminescence (PL) is the

spontaneous emission of light from a material under optical excitation. The samples were measured at spectral range between 390 nm to 590 nm with an excitation wavelength of 350 nm. The excitation energy and intensity are chosen to probe different regions and excitation concentrations in the sample.

PL can be used to characterize a variety of material parameters. PL spectroscopy provides electrical characterization, and is a selective and extremely sensitive probe of discrete electronic states.[8]

4.5 Scanning Electron Microscope (SEM)

The SEM was used to determine the size of the particles and to determine relative morphology. Figure 24 shows the Gemini Leo 1525 SEM. The Accelerating Voltage was 100V to 30KV and the resolving power was 1.5 nm at 20 KV and 3.5 nm at 1 KV. The SEM shows that the particle size is roughly what the manufacturer claimed at 50 nm (difficult to tell due to aggregation of the particles). The morphology did not change in the composite, which means the particles are stable with the carbon coating throughout the manufacturing process. The manufacturing process did include using various solvents in the individual polymers (Polymer A in Xylene and emraldine salt, and Polymer B in Chloroform).

4.6 Capacitance

The capacitance was determined for the samples on the glass substrate and aluminum electrode deposition by using the LCR Meter. Each device has three wires and a ground wire. All three wires were tested and reported in Chapter 5.5. The LCR used Alternating Current at 1 KHz frequency.

4.7 Permittivity

The permittivity was determined by using the capacitance measured on the LCR Meter and the thickness of the polymer film determined by the Ellipsometer, Figure 25. The Ellipsometer's use is annotated in the "Index of Refraction" Chapter) in the following equation;

$$C = \frac{\epsilon A}{d}, \quad (3)$$

where C is capacitance, ϵ is the permittivity, A is the area of the aluminum electrode deposited over the film and the ITO portion of the glass and d is the thickness of the polymer on the glass substrate. Solve for permittivity (ϵ). See Figure 26 for a schematic of the sample.

4.8 Permeability

The relative permeability was calculated by the following equation;

$n = (\mu * \epsilon)^{1/2}$;[3] where n = index of refraction, μ = permeability and ϵ = permittivity.

4.9 Index of Refraction

Optical properties of materials are those characteristic properties that determine the interaction of light with matter; an example being the refractive index, n, that determines the speed of light in a medium n = c/V, where *V* is the speed of light in the medium and *c* is the speed of light in free space.[8]

The index of refraction (also known as refractive index) was needed to calculate the permeability of samples. The index of refraction was measured on a Gaertner Ellipsometer Figure 25 with the wavelength of 632.8 nm (red) laser. The composite was spun cast onto a silica substrate. The samples were each measured at least five times at a different location on the samples and the thickness and the index of refraction were averaged.

Table 2 lists the standard deviation for the testing of the index of refraction. The standard deviation was very small (0.02-0.1). The incidence angle was set at 70 degrees. The index of refraction of the substrate was

entered and then the index of refraction was estimated for the polymer/nanoparticle composite. Most polymers without nanoparticles have an index of refraction in the range from 1.5-1.6. The sample was placed in the instrument and the reference lines were observed through the eye piece. The machine was adjusted to center the reference lines. The platform was adjusted for the strongest reference lines. The platform height was adjusted for the maximum level equal to the digital reference line (in the software). The measurement was taken and the values were recorded for each sample.

CHAPTER 5

Results and Discussion

5.1 FTIR

FTIR *absorbance* spectra of Polymer A and Polymer A plus nanoparticles are shown in Figure 30. The absorption bands between 1500 to 1660 cm^{-1} are attributed to the C=N bonds (conjugated) and C=C (Conjugated) double bond vibrations respectfully, the weak absorption band at 3200 cm^{-1} is attributed to the =NH hydrogen stretching. The absorption bands at 700 cm^{-1}, 1000 cm^{-1}, 1150 cm^{-1} and 1500 cm^{-1} are attributed to the aromatic ring bond vibrations. The absorption band at 2900 cm^{-1} are attributed to the =CH stretching. There are two bands in the region from 2300-2400 cm^{-1} that are attributed to the gas purge. These bands are the result from moisture in the. Analysis of the FTIR data was performed based on studies by Wang et al. These FTIR *absorbance* spectra can be compared to the spectra in the literature (Section 2.4) Figure 8. The *Transmittance* spectra for PANI plus $Zn_{0.6}Cu_{0.4}Cr_{0.5}Fe_{1.5}O_4$ magnetic nanoparticles are in Figure 8.[16] The data is very similar to what was reported in this thesis with the exception of the *absorbance* peak around 2350 wave number (cm^{-1}) which can be attributed to moisture in the sample and the interaction of the instrument to that moisture (this is a well documented phenomena). The FTIR spectrum is compared to the literature in Section 2.5 (Figure 11), the pure PANI

displays the same absorbance bands, but the PANI plus TiO2 nanoparticles displays greater intensity in some bands and their spectral shifts of some bands indicating strong interaction between polymer and TiO2 nanoparticle. There does not appear to be any spectral shifts due to the magnetic nanoparticle, but there is greater intensity in the Polymer A/nanoparticle sample which does indicate an interaction between the Polymer A chains and magnetic nanoparticle. The interaction between polymer and magnetic nanoparticles (dipole-dipole and electron donation) has been discussed in Sections 1.5, 2.8 and 2.9.

FTIR *absorbance* spectra of Polymer B and Polymer B plus nanoparticles are shown in Figure 31. The absorption bands at 2961 cm^{-1} and 2866 cm^{-1} are attributed to the stretching vibration mode of CH_3. The signal at 2925 cm^{-1} is attributed to the stretching vibration mode of CH_2. The signal at 1372 cm^{-1} is attributed to C-CH_3 deformation and the signal around 1465 is attributed to -CH_2- deformation. There was not a discernable peak for the C-S bond and the literature does mention it will be a very slight peak. A Spectral comparison of the IR values between the pure Polymer B sample and Polymer B plus nanoparticles shows slightly differences in intensities. This phenomenon could possibly be attributed to the extra carbon that is covering the nanoparticles. In the Polymer B sample there is not a noticeable difference between the two spectra (pure Polymer B and Polymer B with nanoparticles). This would signify that there is

little interaction between nanoparticle and polymer using FTIR. Analysis of the FTIR data was performed using reference 23.

Due to the higher mass of the nanoparticle atoms, vibrations of transitional metal–oxygen bonds appear in the far-infrared region, characteristic peaks of the nanoparticle cannot be expected in the present spectral window.[23]

Other forms of spectroscopy do show that there is a definite interaction between polymer and magnetic nanoparticle in both the Polymer A and Polymer B samples, such as UV-Vis spectroscopy.

5.2 Ultra Violet-Visible Spectrometer

Colored substances owe their color to the presence of conjugated unsaturated linkages.[24] These linkages conferring color on substances are called chromophores. Some groups conferring color on a substance are found to increase the coloring power of a chromophore. Such groups are called auxochromes. Typical examples of chromophores are, C=C, C=O, N=N etc. Examples of auxochromes are, C-Br, C-OH, C-NH_2 etc.[24]

Figure 33 and Figure 34 show the UV-Vis Absorption Spectra of the polymers. The Electromagnetic spectrum is Figure 35 for ease of reference with the colors associated with the polymers. The Polymer A does not absorb the green wavelengths due to the complex chromophore of the benzene rings (an observed trough around 525 nm, Figure 33).[24]

The Polymer A UV-Vis graph does compare favorably to the literature in Section 2.4. Figure 7 is a graph of PANI plus $Zn_{0.6}Cu_{0.4}Cr_{0.5}Fe_{1.5}O_4$ magnetic nanoparticles. It shows two peaks that shift to increasing wavelengths with an increase in the magnetic nanoparticles. The peaks are around 350 nm and 625nm. Figure 33 shows a similar peak shift from this thesis research. The peak shift is from pure polymer to the polymer plus nanoparticles. The shift continues to longer wavelengths with increasing nanoparticle weight. These results suggest there is an interaction between the polymer and magnetic nanoparticle.

The interaction between polymer and magnetic nanoparticles (dipole-dipole and electron donation) has been discussed in Section 1.5 and also Literature Review Sections 2.8 and 2.9.

The Polymer A UV-Vis graph does not compare favorably to the literature in Section 2.5. The UV-Vis spectra for PANI plus TiO_2 are in Figure 10. The reason the two spectra are vastly different is due to the literature's not reporting pure PANI in the UV-Vis spectra. The literature data does have peak shifts indicating the strong interaction between polymer and TiO_2.

The Polymer B UV-Vis Spectra are presented in Figure 34, Polymer B has the C=C chromophore that is responsible for its coloring.[24] The Polymer B UV-Vis graph does show shifting as well from the pure Polymer B to Polymer B with nanoparticles which also is indicative of interaction between the polymer and the

nanoparticles. There was no reported investigation literature that used Polymer B and magnetic nanoparticles.

The interaction between polymer and magnetic nanoparticles (dipole-dipole and electron donation) has been discussed in Section 1.5 and also Literature Review Sections 2.8 and 2.9.

5.3 Photoluminescence (PL)

The PL data for the samples can be seen in the following figures; Figure 36 and Figure 37.

The Polymer A samples have substantial excitation of photons in the wavelength from 415 nm to 430 nm for all samples. Refer to Figure 36 for peaks associated with the Polymer A samples. There is a peak shift (the excitation peak moves to lower wavelengths) from the pure sample and samples with magnetic nanoparticles and the sample with the most nanoparticles has the greatest shift. Again this indicates an interaction between the polymer chain and the magnetic nanoparticle.

Note: The interaction between polymer and magnetic nanoparticles (dipole-dipole and electron donation) has been discussed in Section 1.5 and also Literature Review Sections 2.8 and 2.9.

The Polymer B samples have excitations in the range of 415 nm to 430 nm for samples with nanoparticles and for the pure Polymer B sample 540 nm to 565 nm. There is a huge peak shift (the excitation peak moves to lower

wavelengths) from the pure Polymer B to the Polymer B with Nanoparticles which is indicative of a strong polymer chain interaction with the magnetic nanoparticle during photoluminescence excitation.

The interaction between polymer and magnetic nanoparticles (dipole-dipole and electron donation) has been discussed in Section 1.5 and also Literature Review Sections 2.8 and 2.9.

5.4 SEM

The carbon coated nanoparticles tend to aggregate as evident in Figure 38 (Polymer A with nanoparticles). During preparation the composites were measured and then placed in a sonic mixer for several minutes prior to spin casting the samples. The nanoparticle size can be determined roughly to be around 50 nm by the SEM. There was some good dispersion in the Polymer A samples as is evident in Figure 39. There was some undulation in the film associated with the spin casting of the sample probably due to the high viscosity of the polymer in solution plus nanoparticles (the nanoparticles can increase viscosity), Figure 40. Polymer B with nanoparticles is in Figure 41.

The literature has two SEM micrographs of PANI and $Zn_{0.6}Cu_{0.4}Cr_{0.5}Fe_{1.5}O_4$ shown in Figure 9. The literature's scale is 500 nm and this thesis scale is either 1000 nm or 2000 nm (refer to the legend on the figure for scale). The morphologies are clearly different between the nanoparticles and the $Zn_{0.6}Cu_{0.4}Cr_{0.5}Fe_{1.5}O_4$ nanoparticles.

5.5 Capacitance Determination

The sample capacitance is listed in Figure 32. Sample A15 has the highest capacitance of all the samples at 8.3 nano Farads (nF). The lowest capacitance is Sample is E5 at 0.66 nF. The equation for capacitance is $C = \frac{\epsilon A}{d}$.(3)

5.6 Permittivity

Permittivity for the samples is located in Figure 28. Figure 27 has permittivity plotted with data from the literature in Chapter 2.3. The polymers displayed very high permittivity for polymers. (Typical polymers are on the order of 2-12 for relative permittivity ε_r.) The Polymer B sample (A15) with 15% (by weight) nanoparticles displayed the highest permittivity at 38.12. The literature reports similar values for permittivity (Chapter 2.3) with their highest value for permittivity at 32. The data in the literature uses higher percent by weight of nanoparticles. In this thesis the maximum percent of nanoparticle is 15% where the literature goes up to 50% nanoparticles. The values for permittivity for this thesis range from 5.45 to 38.12.

The nanoparticles were coated with carbon for stability purposes. The literature goes into depth as to why the nanoparticles were coated (Chapter 2.10)

The manufacturability of the Polymer A and Polymer B samples with nanoparticles is much easier than trying to make flakes out of the nanoparticles and then coating them with silica. The data displays that Polymer A and Polymer

B are definitely a better polymer choice for high permittivity than PS or PMMA with Fe nanoparticles. The flake structure does allow for less eddy current loss per the literature so it might be beneficial to look into milling the nanoparticles into flake form to increase the permeability.

5.7 Permeability

The values for permeability are indeterminate from the method used to calculate it (from the index of refraction). There were no instruments available to measure the permeability directly from the sample. The values expected for permeability are listed in the literature (Chapter 2.3). Typical values should be in the range of 5-22 for relative permeability increasing with increasing nanoparticle percentage.[15] The values for permeability were computed with the following equation; $n = (\mu * \epsilon)^{1/2}$;[3] where n = index of refraction, μ= permeability (relative) and ϵ = permittivity (relative). The samples should be tested on an instrument to determine the values of permeability for the samples.

5.8 Index of Refraction

Figure 29 shows the index of refraction for the samples (Table 2 lists the standard deviation of the samples taken). The index of refraction was used to

determine permeability for the samples. $n = (\mu * \epsilon)^{1/2}$;[3] where n = index of refraction, μ= permeability (relative) and ϵ = permittivity (relative).

The Polymer A samples displayed increasing index of refraction for increasing nanoparticles (percent by weight from 5%-15%), which is to be expected. The values for index of refraction range from 2.16 to 2.31.

The Polymer B samples also showed an increase in the index of refraction for an increase in nanoparticles (percent by weight from 5%-15%). The range of index of refraction for the Polymer B samples is 2.3 to 2.65.

The increasing index of refraction is another indicator that the nanoparticles are interacting with the polymer chains.

Note: The interaction between polymer and magnetic nanoparticles (dipole-dipole and electron donation) has been discussed in Chapter 1.5 and also Literature Review Chapters 2.8 and 2.9.

5.9 Microwave Absorption

The microwave absorption was not calculated/measured due to lack of local capability. Microwave absorption is dependent on high loss energy materials. High Loss energy refers to the ability to absorb the incident radiation and dissipate it as heat.[20] The manufacture of high loss energy materials basically involves the use of compounds capable of generating dielectric and/or magnetic

losses (absorption) when impinged by an electromagnetic wave. Conducting polymers are a class of high loss energy materials that show a number of advantages over traditional granular materials, presenting high conductivity combined with light weight.[20] The microwave absorption was measured in the literature (Chapters 2.2, 2.9 & 2.10). The iron flake nanoparticles resulted with more absorption with more nanoparticles. In Chapter 4.9 the authors performed the research for applications in electronic magnetic interference shielding and broadband microwave absorbing material.[21] Chapter 2.10 discusses the complex permeability steadily increases with an increase in magnetic nanoparticle. Figure 13 is the graph that shows the complex permeability can be described as transforming the microwave into heat dissipation and therefore reflecting less of a signal than the original signal. The data supports the conclusion that more magnetic nanoparticles reflect fewer microwaves than the original intensity.[22]

Since the research in the literature is similar to the thesis work, I would postulate the microwave absorbance for the Polymer A/nanoparticles and the Polymer B/nanoparticles would increase with increasing nanoparticles. Further testing needs to be conducted in this area.

CHAPTER 6

Conclusions and Recommendations

6.1 Conclusions

The research has successfully produced two conducting polymer composites with high permittivity and most likely high permeability and high microwave absorption characteristics. This success could be used for device miniaturization and other electrical applications. The sample preparation is relatively simple with no products susceptible to explosion in an oxygen environment.

Polymer A displayed high permittivity, but had poor optical properties (transmittance/absorbance) due to the thickness of the polymer in the samples used. Polymer A also had a definite interaction between polymer chains and nanoparticles as evident in the UV-Vis graph and photoluminescence.

New samples were made with thinner film, but the chromophores are very distinct with a dark green hue and, therefore, would have to be made into a very thin film to be of use with the optics in mind.

Polymer B displayed high permittivity with good optical properties (transmittance/absorbance) and a definite interaction between polymer chains and nanoparticles as evident in the UV-Vis graph and photoluminescence.

6.2 Recommendations

To increase the permeability of the samples three methods need to be researched;

1. More nanoparticles in the samples (increase the weight by percent of nanoparticles in the sample). Samples can be made with 30%, 40% and 50% weight fractions and the same values can be measured to determine if permeability increases.
2. Possible milling the nanoparticles into flakes. One source wrote the maximum permeability with spherical nanoparticles is 3.0 regardless of the amount of particles added to the composite.[15] Those results were only reported in one of the references that was researched for the thesis.
3. Better dispersion techniques. There was notable aggregation with the particles in the samples. Further research needs to be performed to equally distribute the nanoparticles throughout the polymer. The nanoparticles did come in a powder form and one manufacturer of nanoparticles wrote;

   Many of these nanomaterials are made directly as dry powders, and it is a common myth that these powders will stay in the same state when stored. In fact, they will rapidly aggregate through a solid bridging mechanism in as little as a few seconds. Whether these aggregates are detrimental will depend entirely on the application of the nanomaterial. If the nanoparticles

need to be kept separate, then they must be prepared and stored in a liquid medium designed to facilitate sufficient interparticle repulsion forces to prevent aggregation.[4]

A possible solution could be to leave in a mixer until they are ready to be spun cast and immediately place on the substrate and spin the sample before the nanoparticles can aggregate. A better distribution should increase the permeability of the samples so there is not only a local magnetic effect but a macro magnetic effect over the whole sample. Also, if the nanoparticles were added to the substrate in a magnetic field to align the nanoparticles that could possibly increase the permeability.

At present there is no access to instruments that directly measure the permeability of a sample. This value would need to be measured to gain insight into how the increases in nanoparticles affect the value for permeability.

At present there is no access to instruments that measure the Dielectric Loss. The real and complex permittivity would need to be measured for each sample and I would hypothesize that it would, indeed, be a low value for the polymer composites. The low Dielectric loss would mean low heat from the samples when a current was applied. This benefit is obvious in electronics when heat dissipation is always a problem.

New samples of Polymer A with nanoparticles need to be manufactured diluted with Xylene to make the films even thinner than the second samples,

which were diluted, so they display better optical properties (better transmittance). If the film was thin enough, the film could be used to coat canopies, pilot helmets, optical sensors, displays, etc.[18]

All the samples should be tested for microwave absorption due to their magnetic properties and current interest by the military for microwave absorbing materials.

All the samples should be tested for time degradation to see if these properties will change over time and if further research is needed to maintain their original permittivity and permeability of the samples.

Preparation of the samples for the UV-Visible spectrometer should be done on quartz substrate to observe the UV absorbance for the polymer samples, if that region of electromagnetic spectrum is of interest to the community.

LIST OF REFERENCES

(1) Sperling, L.. Physical Polymer Science. New York: Wiley-Interscience, 2001.

(2) Nobel, "NobelPrize.org". The Nobel Prize in Chemistry 2000. 19 February 2009 < http://www.nobel.se/chemistry/laureates/2000/index.html>.

(3) Kasap, S.. Electronic Materials and Devices. New York: McGraw-Hill, 2002.

(4) "Malvern Innovative Solutions in Material Characterization". Malvern. 2 April 2009<http://www.malvern.com/LabEng/industry/nanotechnology/nanoparticle_defiition.htm>.

(5) "Polymer Composites as Construction Materials". DTI. 14 April 2009 <http://www.polymercomposites.co.uk/>.

(6) Bolton, B.. "AI Polymer Laminates for High Temperature Stability ". Polymer Engineering and Science Aug 25, 2004: 227-230.

(7) Ivanov, V.. Radiation Chemistry of Polymers. VSP, 1992.

(8) Raju, Gorur. Dielectrics in Electric Fields. New York: Marcel Dekker, 2003.

(9) Exner, Otto. Dipole Moments in Organic Chemistry. Stuttgart: Georg Thieme , 1975.

(10) Roy, Nelson, MacCrone, Schadler, M., J.K., R.K., L.S.. "Polymer Nanocomposite Dielectrics – The Role". IEEE Transactions on Dielectrics and Electrical Insulation 2005: 629-643.

(11) Lu, Salabas, Schuth, An-Hui, E.L., Ferdi. "Magnetic Nanoparticles: Synthesis, Protection, FUnctionalization". Magnetic Nanoparticles 2007: 1223-1240.

(12) Kit, Kevin, “MSE 543 Basic Polymer Physics” 2008:Class Notes

(13) Skoog, et al. Principles of Instrumental Analysis. 6th ed. Thomson Brooks/Cole. 2007

(14) Kim, Sung-Soo et al. "Magnetic, Dielectric, and Microwave Absorbing Properties of Iron Particles Dispersed in Rubber Matrix in Gigahertz Frequencies". Journal of applied Physics 97 10 May 2005: 10F905-1-10F905-3.

(15) Zhang, Xiaokai et al. "High Frequency Properties of Polymer Composites Consisting of Aligned Fe Flakes". Journal of Applied Physics 25 April 2006: 08M914-08M914-3.

(16) Jiang et al., Jing. "Polyaniline/magnetic ferrite nanocomposites obtained by in Situ Polymerization". Reactive and Functional Polymers 2007: 57-62.

(17) Li, Wang, Li, Lu, Xingwei, Gengchao, X., D.. "Surface properties of polyaniline/nano-TiO2 composites". Applied Surface Science 1 Apr 2004: 395-401.

(18) Bunning, Tim. "Polymer Nano-Layer Coatings for Optical Applications". AFRL NanoScience Technologies Applications, Transitions and Innovations 9 February 2009: 26-26.

(19) Wang, Bi, Liu, Sun, Wu, "Magnetic and Microwave Absorbing Properties of Polyaniline/y-Fe2O3 Nanocomposites". Science Direct 2008: 2132-2139.

(20) Lu, Salabas, Schuth, An-Hui, E.L., Ferdi. "Magnetic Nanoparticles: Synthesis, Protection and Functionalization,". Magnetic Nanoparticles 2007: 1223-1240.

(21) Li, et al., Yuan-xun. "Synthesis and Electro-magnetic Properties of Polyaniline-barium Ferrite". Chinese Journal of Chemical Physics Dec 27, 2007: 739-742.

(22) Yongbao et al., Feng. "Complex Permeability and Permittivity and Microwave Absorption Property of Barium Ferrite/EPDM Rubber Radar Absorbing Materials in 2-18GHz ". IEEE 2005: 1-4.

(23) Bellamy, L.J.. The Infrared Spectra of Complex Molecules Volume One. London: Chapman and Hall, 1986.

(24) RAO, C.N.R.. Ultra-Violet and Visible Spectroscopy Chemical Applications. Butterworths: New York Plenum Press, 1967.

(25) Sigma-Aldrich, "Sigma-Aldrich". Sigma-Aldrich. 19 February 2009 <http://http://www.sigmaaldrich.com/united-states.html>.

(26) Antonine Education Website, "What Are the Uses and Hazards of Waves That Form the Electromagnetic Spectrum?". Antonine Education. 23 March 2009 <http://images.google.com/imgres?imgurl=http://www.antonine-

education.co.uk/physics_gcse/Unit_1/Topic_5/em_spectrum.jpg&imgrefurl=

http://www.antonine-ducation.co.uk/physics_gcse/Unit_1/Topic_5/topic_5_=what_are_the_uses_

and_ha.htm&usg=__5SRHRLISMKQwFaxiv_gkKS_UEHs=&h=389&w=619&sz=29&hl=en&start=9&um=1&tbnid=g9mJO

DrVrQ-cOM:&tbnh=85&tbnw=136&prev=/images%3Fq%3

Delectromagnetic%2Bspectrum%26hl%3Den%26rlz%3D1T4GGLL_enUS315US315%26sa%3DX%26um%3D1>.

APPENDIX

FIGURES

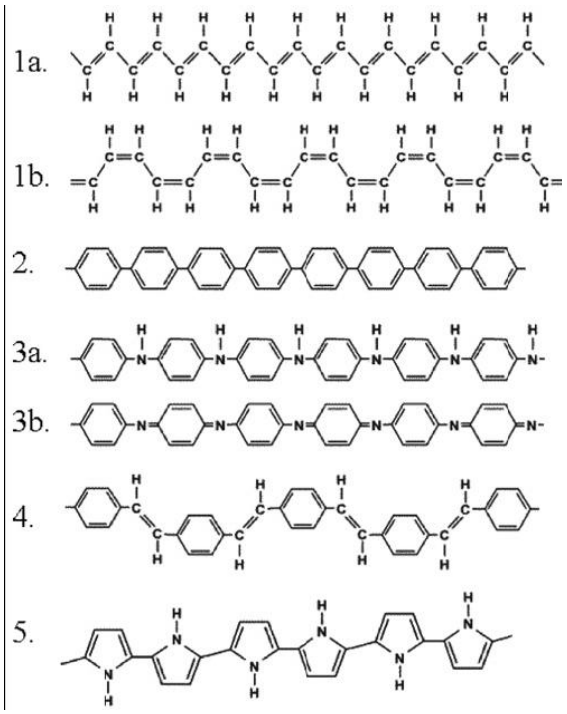

Figure 1. Some conducting polymers: (1) polyacetylene, (2) poly-p-phenylene, (3) polyanilene, (4) polyphenylenevinylene, (5) polypyrrol.[1]

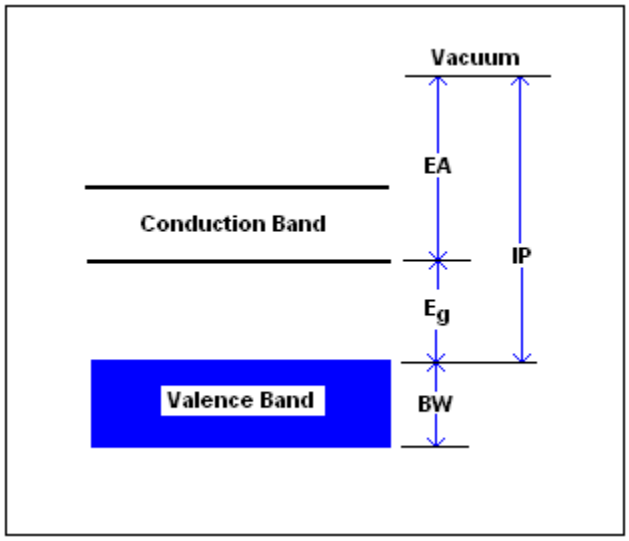

Figure 2. Polymer π-electron band structure. E_g represents the optical bandgap; BW is the bandwidth of the fully occupied valence band; EA is the electron affinity; and IP is the ionization potnetial. [1]

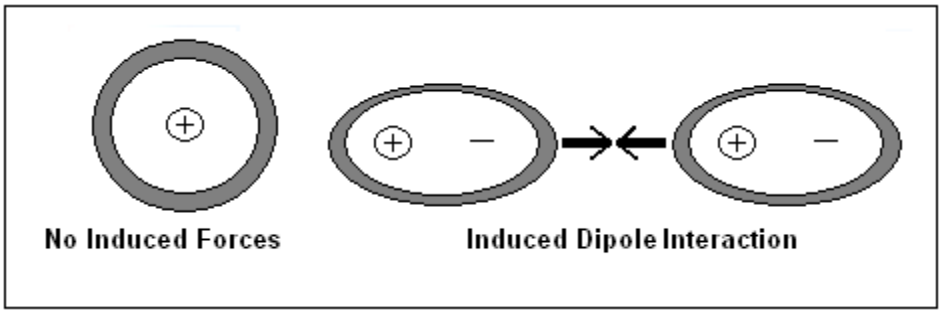

Figure 3. Induced Dipole[3]

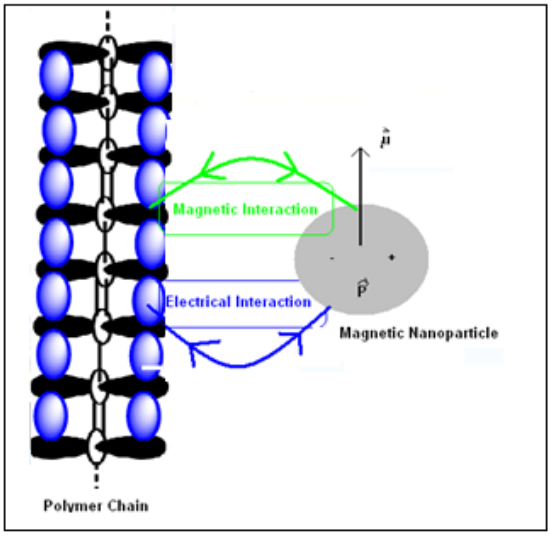

Figure 4. Interactions between polymer chain and magnetic Nanoparticle

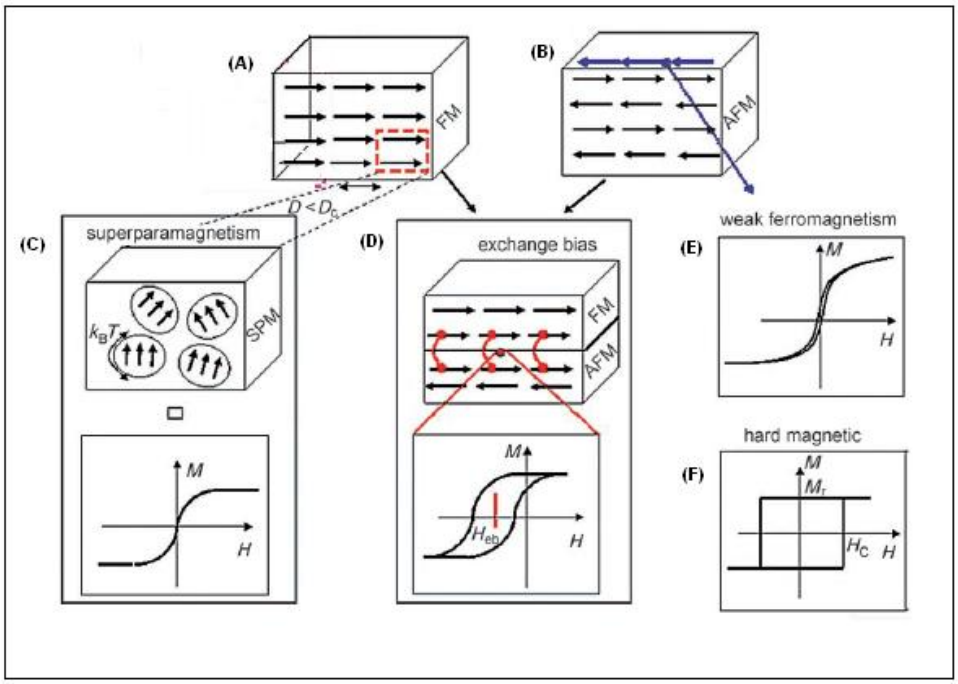

Figure 5. Different Magnetic Effects Occurring In Magnetic Nanoparticles.[20]

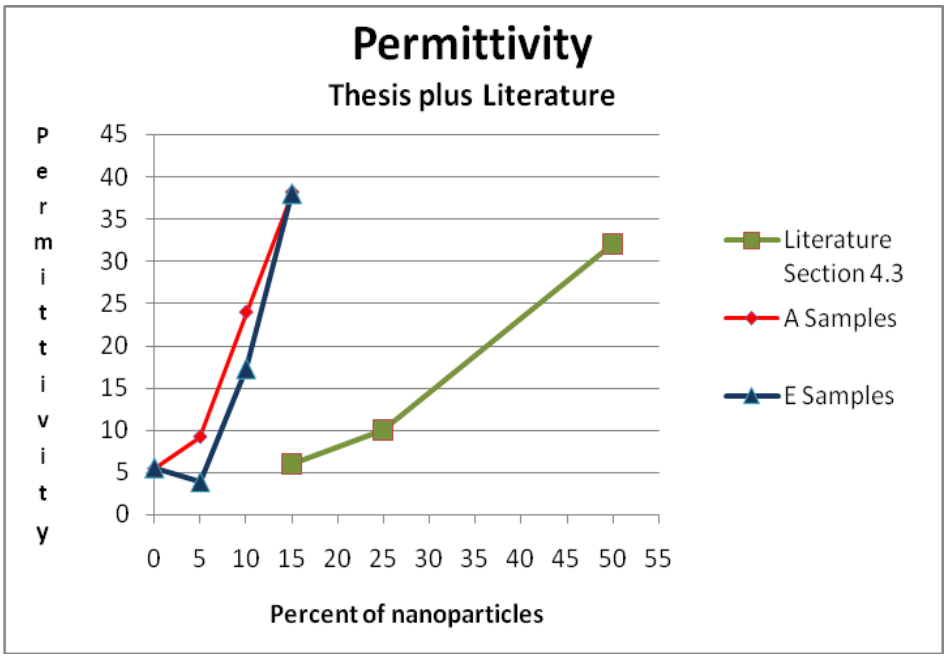

Figure 6. Permittivity of samples A and E and samples from the literature[10]

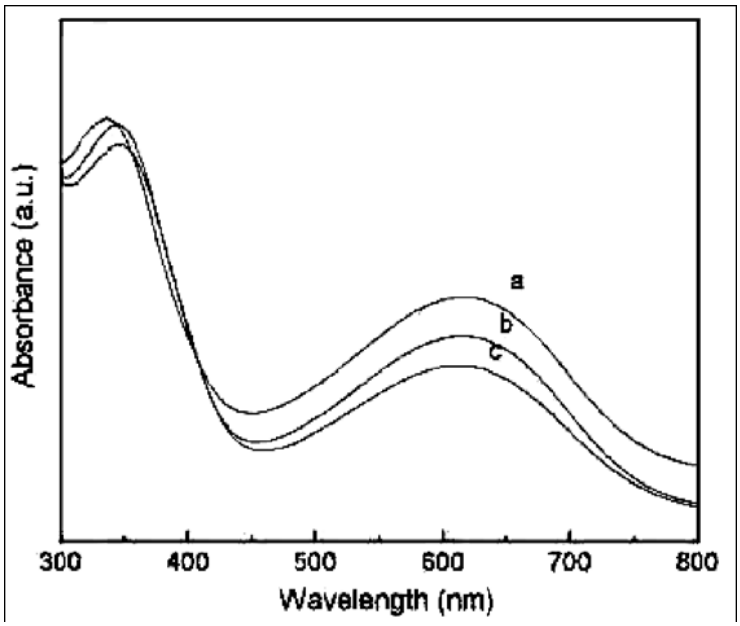

Figure 7. UV–Vis spectra of (a) PANI, PANI–Zn0.6Cu0.4Cr0.5-Fe1.5O4 nanocomposites containing: (b) 10 wt% and (c) 20 wt% Zn0.6Cu0.4Cr0.5Fe1.5O4 particles.[11]

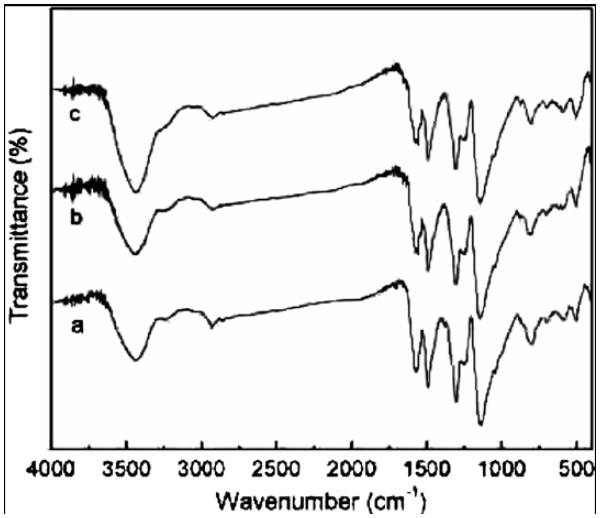

Figure 8. IR spectra of (a) PANI, PANI–$Zn_{0.6}Cu_{0.4}Cr_{0.5}Fe_{1.5}O_4$ nanocomposites containing: (b) 10 wt% and (c) 20 wt% $Zn_{0.6}Cu_{0.4}Cr_{0.5}Fe_{1.5}O_4$ particles. [11]

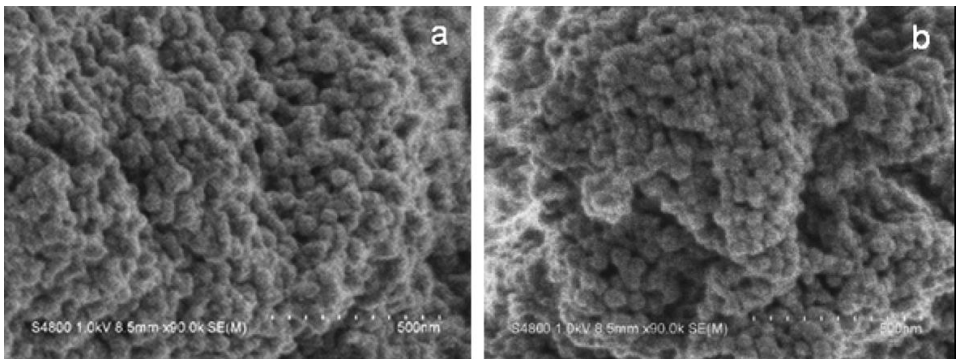

Figure 9. SEM images of PANI–$Zn_{0.6}Cu_{0.4}Cr_{0.5}Fe_{1.5}O_4$ nanocomposites containing: (a) 10 wt% and (b) 20 wt% $Zn_{0.6}Cu_{0.4}Cr_{0.5}Fe_{1.5}O_4$ particles.[11]

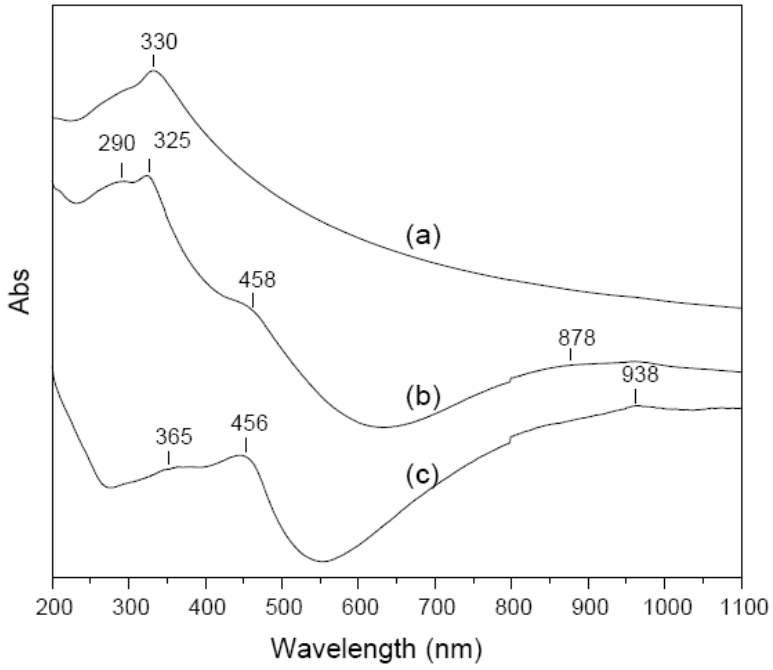

Figure 10. UV-Vis absorption spectra of (a) nano-TiO2 particles, (b) polyaniline/nano-TiO2 composite and (c) doped polyaniline.[17]

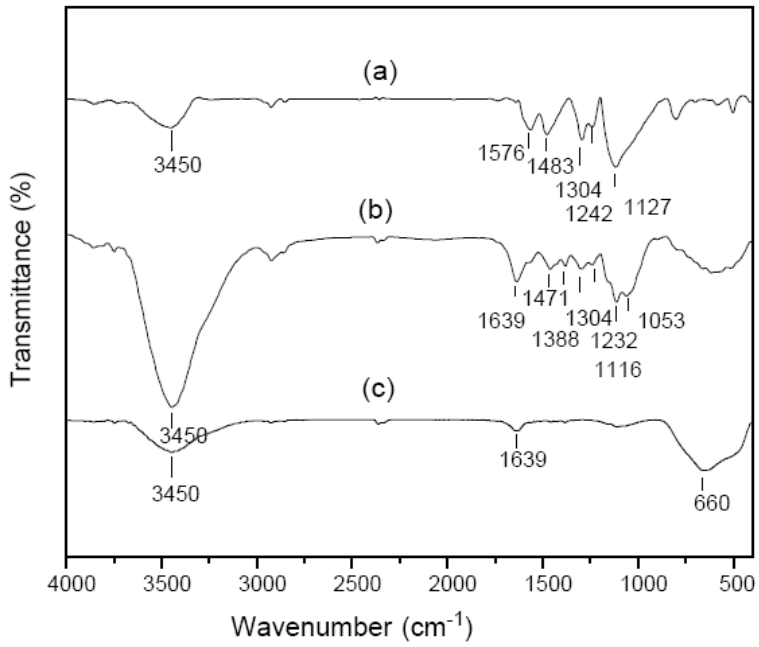

Figure 11. Fourier-transform infrared spectra of (a) doped polyaniline, (b) polyaniline/nano-TiO2 composite (c) and nano-TiO2 particles. [17]

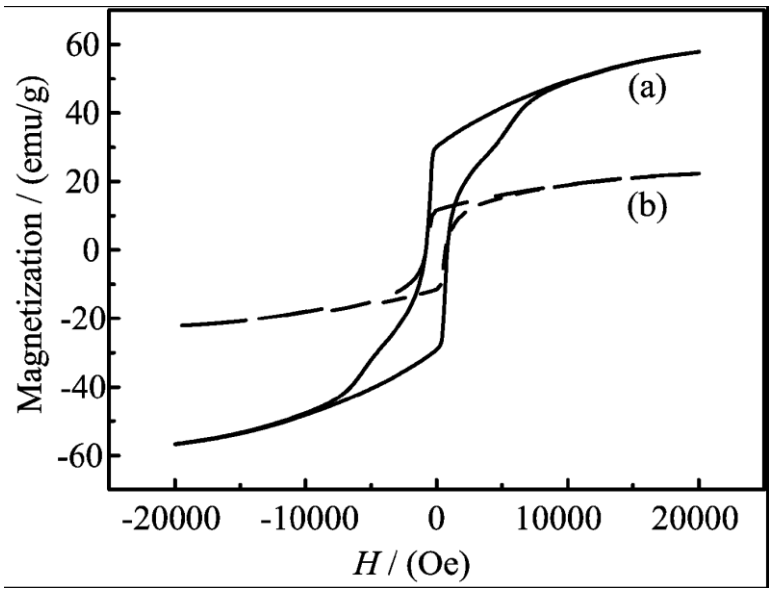

Figure 12 Magnetic hysteresis loops of $BaFe_{12}O_{19}$ (a) and 50% PANI-barium ferrite composite (b).[21]

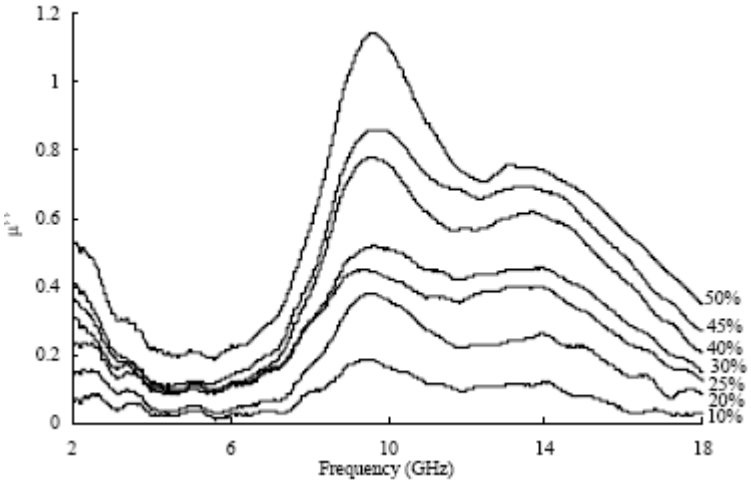

Figure 13. The complex permeability spectra of the RAM with various ferrite volume fractions.[22]

Figure 14. Fisher Vacuum Oven Model 281

Figure 15. Locally Fabricated Spin Cast Machine

Figure 16. Cooke Vacuum Aluminum Deposition Vaporizer

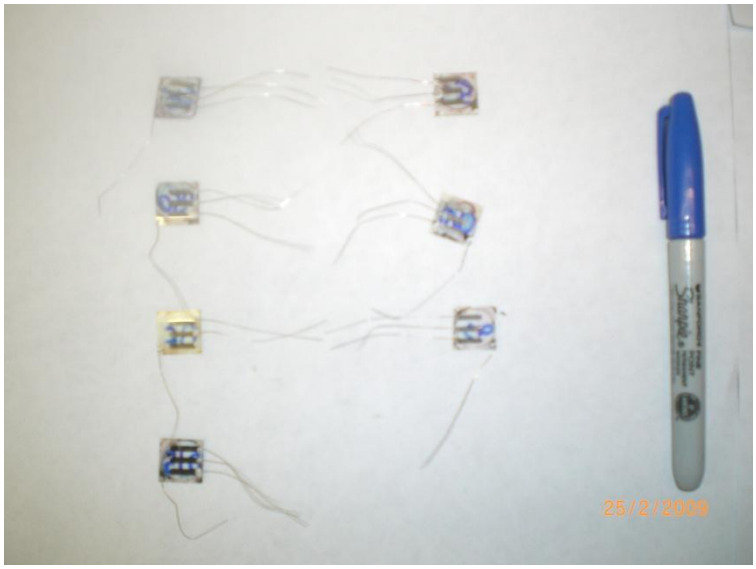

Figure 17. Samples with Aluminum Evaporated Electrodes

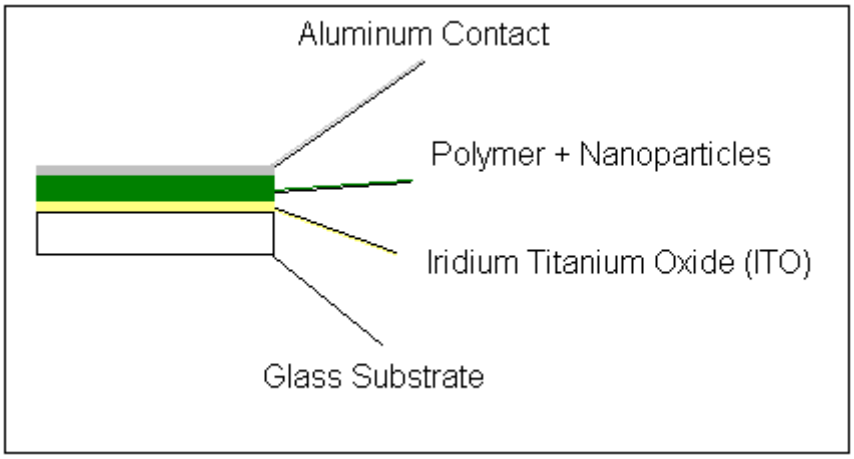

Figure 18. Schematic of Glass Substrates

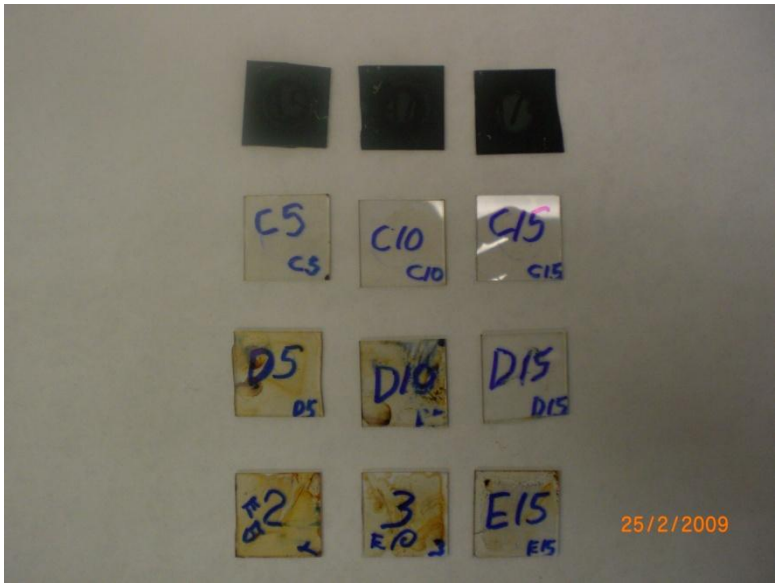

Figure 19. Samples without Aluminum Electrodes

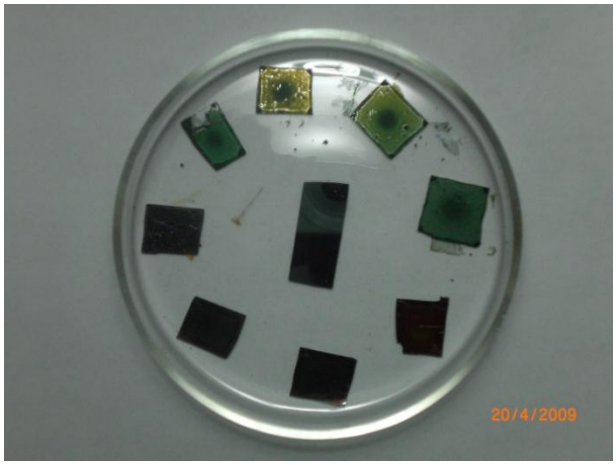

Figure 20. Samples on silica substrate.

Figure 21. Fourier Transform Infrared Spectrometer

Figure 22. Lambda 35 Ultra-violet/Visible Spectrometer

Figure 23. Fluorolog Photoluminescence Measuring Instrument

Figure 24. Gemini Leo 1525 Scanning Electron Microscope

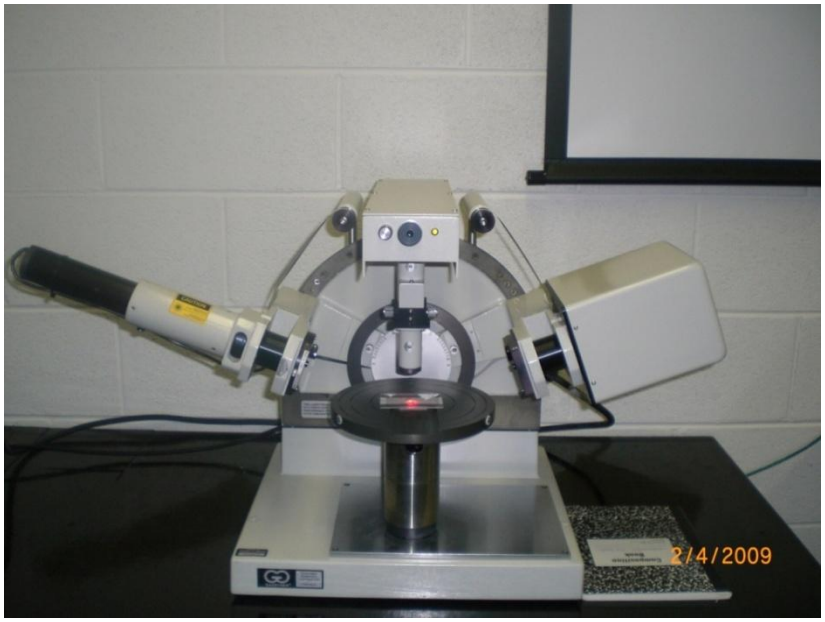

Figure 25. Gaertner Ellipsometer

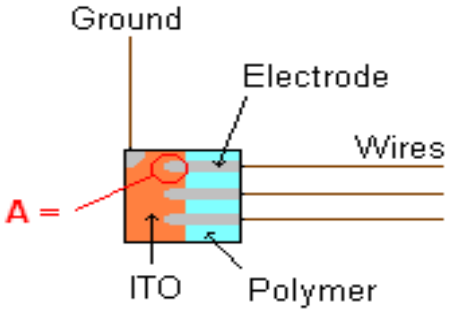

Figure 26. Schematic Of Area To Be Used In Calculation For Permittivity

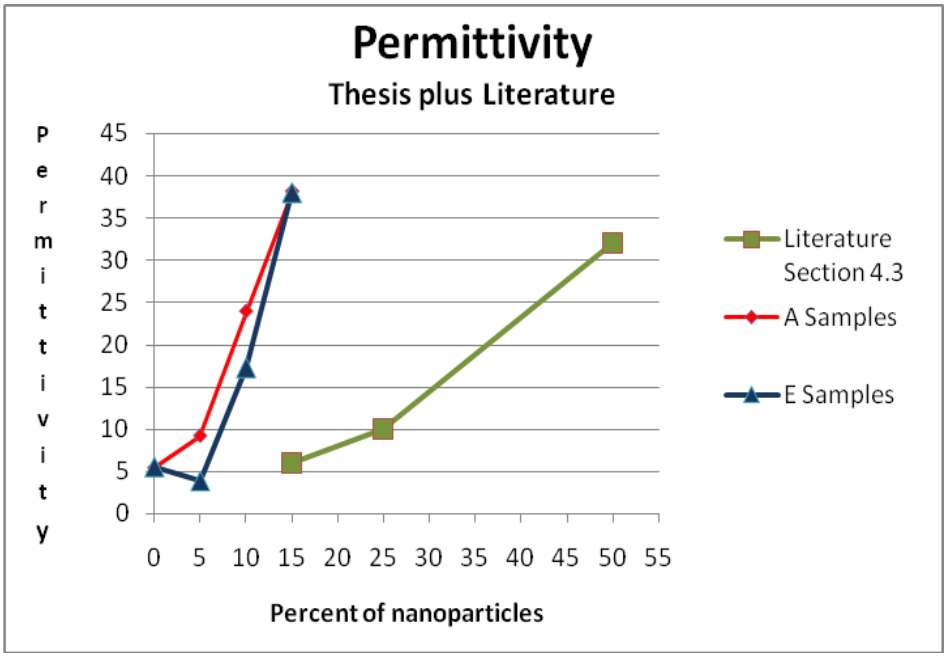

Figure 27. Permittivity of samples A and E and samples from the literature[10]

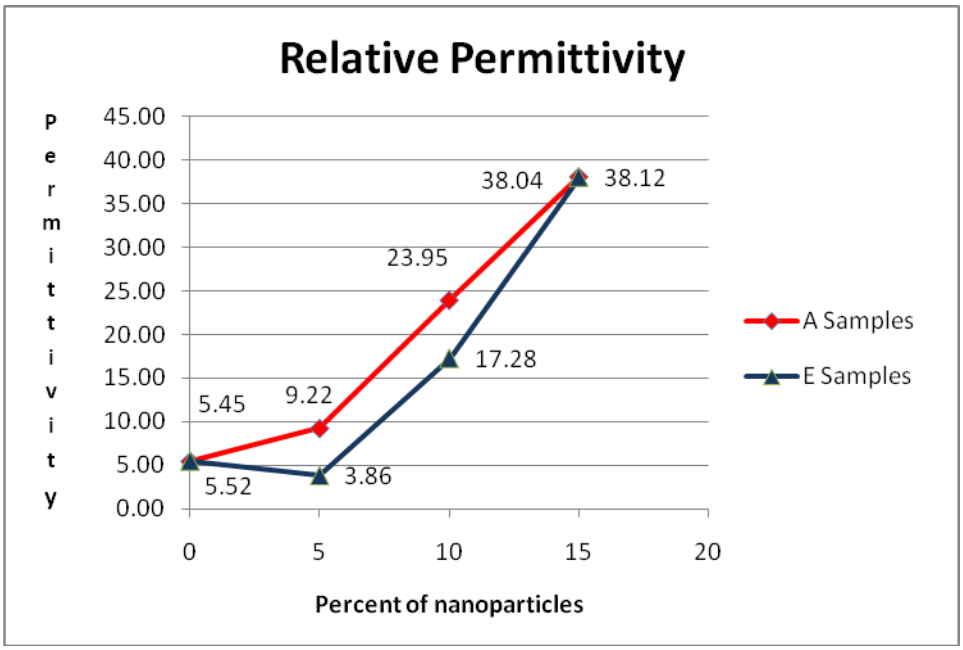

Figure 28. Relative Permittivity Samples A and E

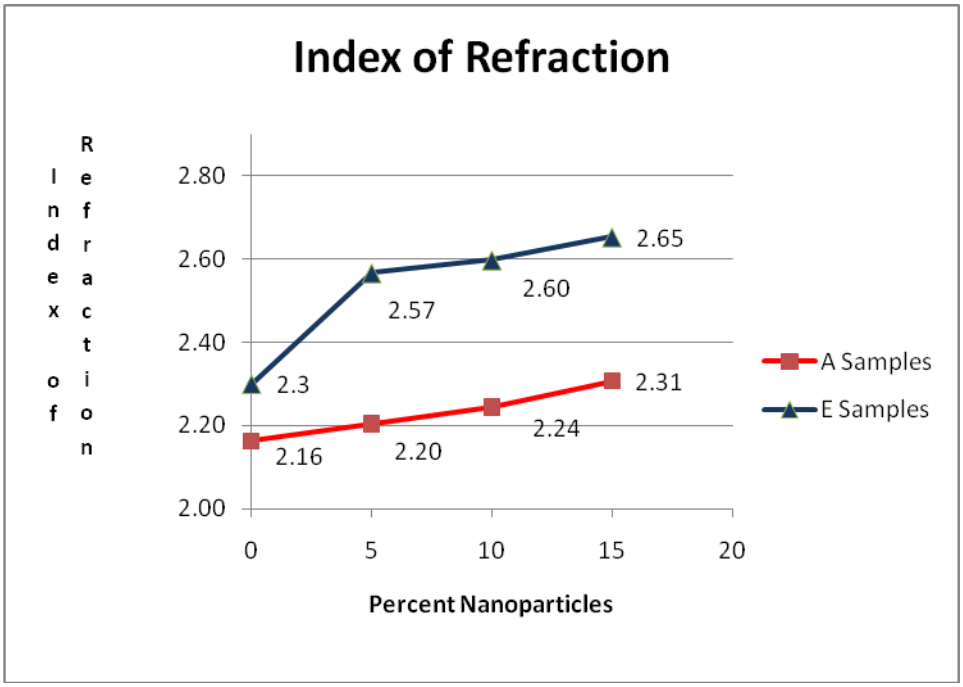

Figure 29. Index of Refraction for samples A and E

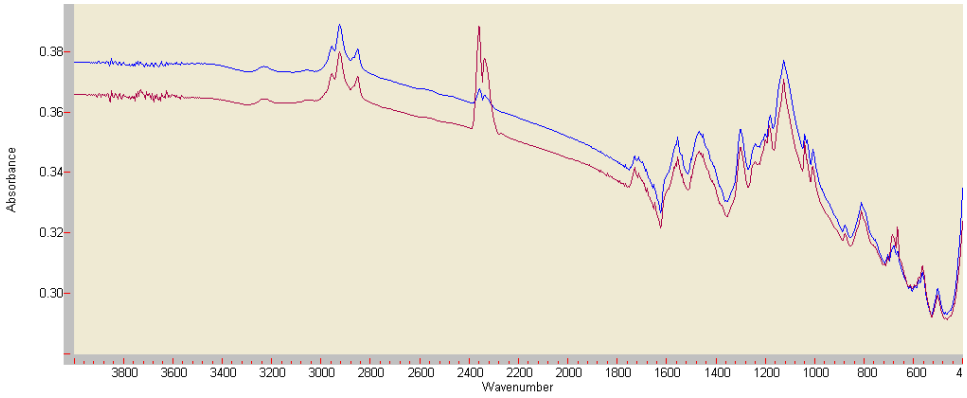

Figure 30. FTIR Data for; Polymer A plus Nanoparticles (Blue line) and Pure Polymer A (Red line)

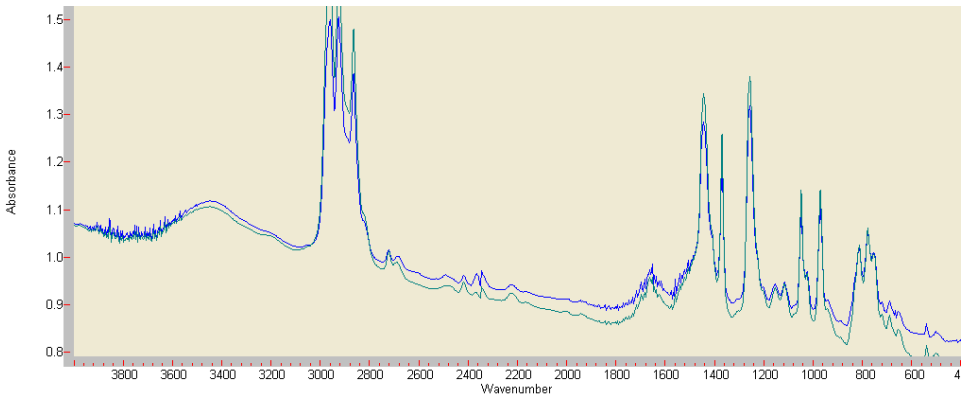

Figure 31. FTIR Data for; Polymer B plus Nanoparticles (green line) and Pure Polymer B (blue line)

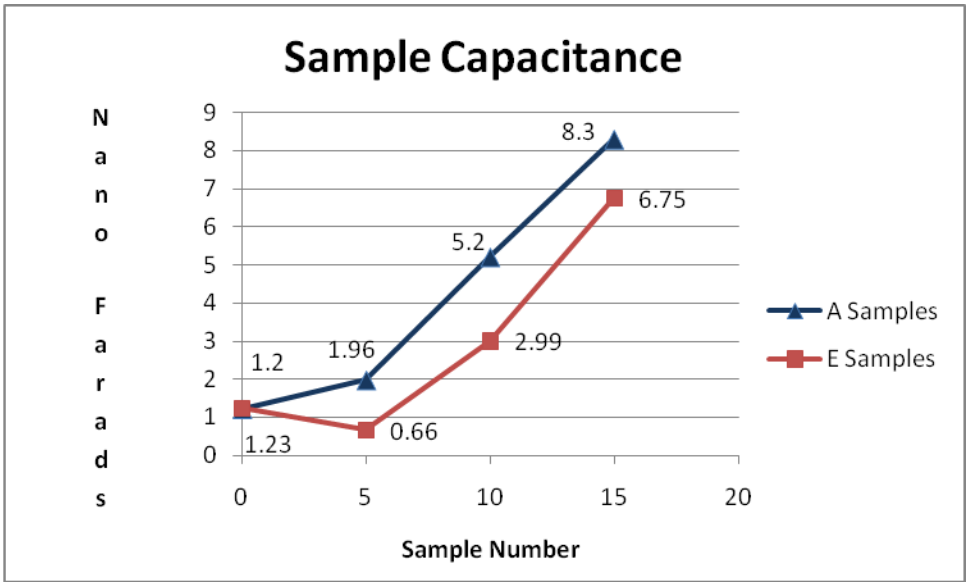

Figure 32. Capacitance of samples

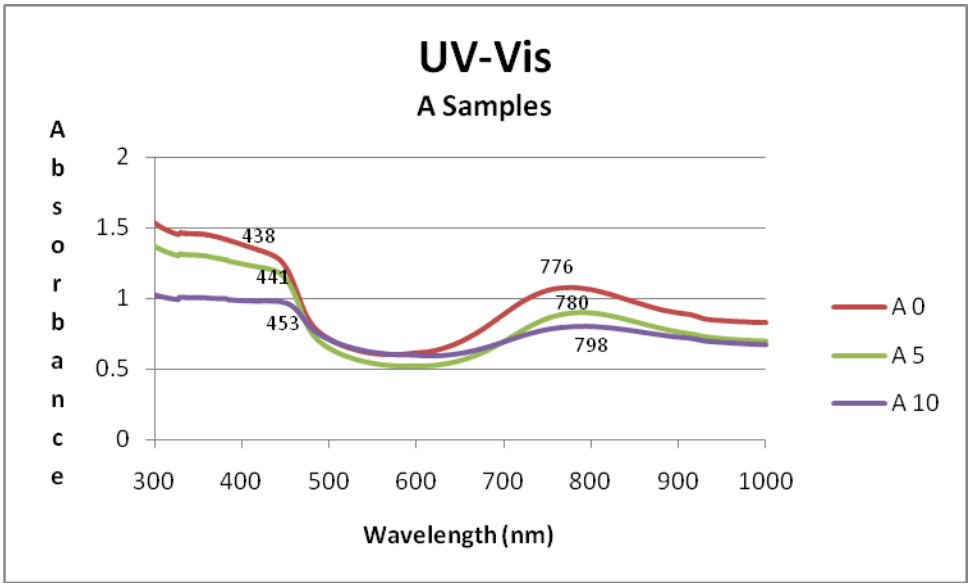

Figure 33. UV-Vis Data for Polymer A with Different Weight Fractions of Nanoparticles; A 0 (0% nanoparticles), A 5 (5% Nanoparticles), A 10 (10% Nanoparticles)

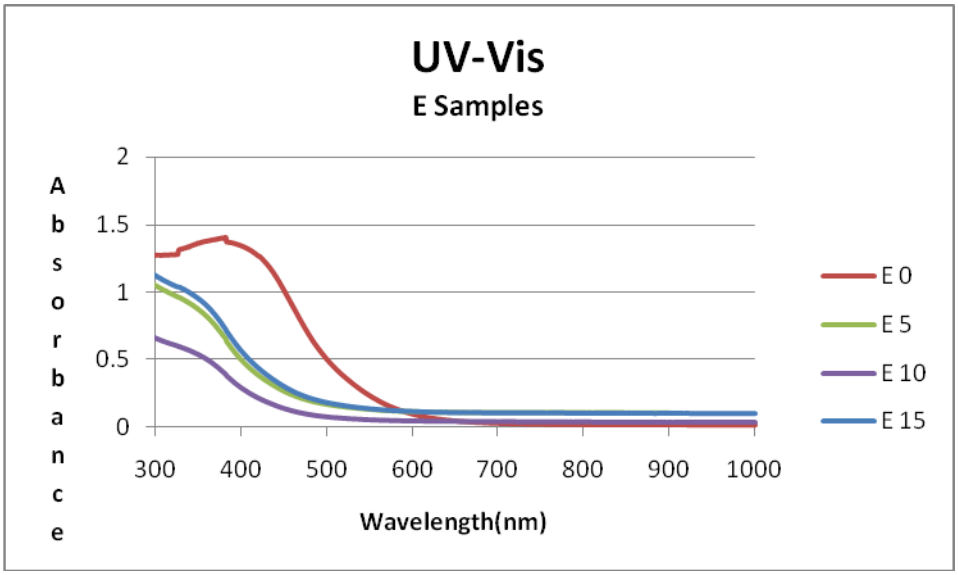

Figure 34. UV-Vis Data for Polymer B with Different Weight Fractions of Nanoparticles; E 0 (0% nanoparticles), E 5 (5% Nanoparticles), E 10 (10% Nanoparticles), E 15 (15% Nanoparticles)

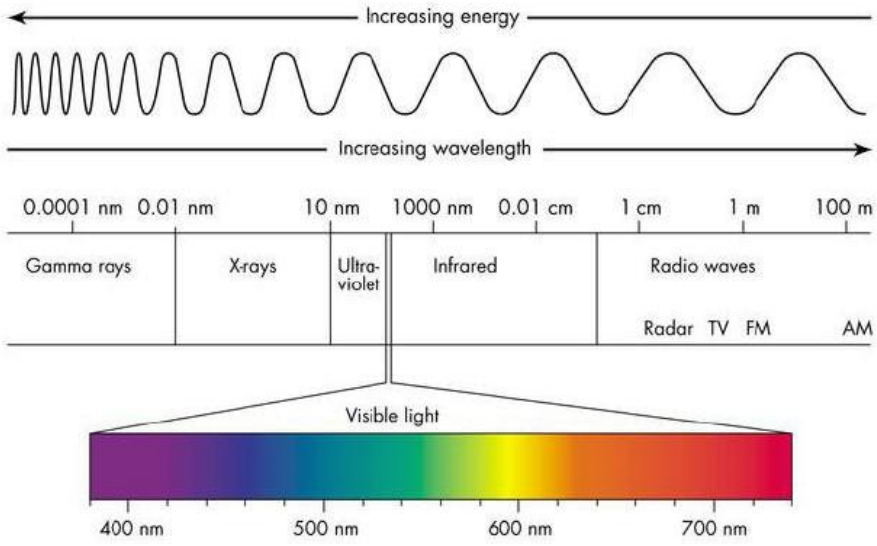

Figure 35. Electromagnetic Spectrum[18]

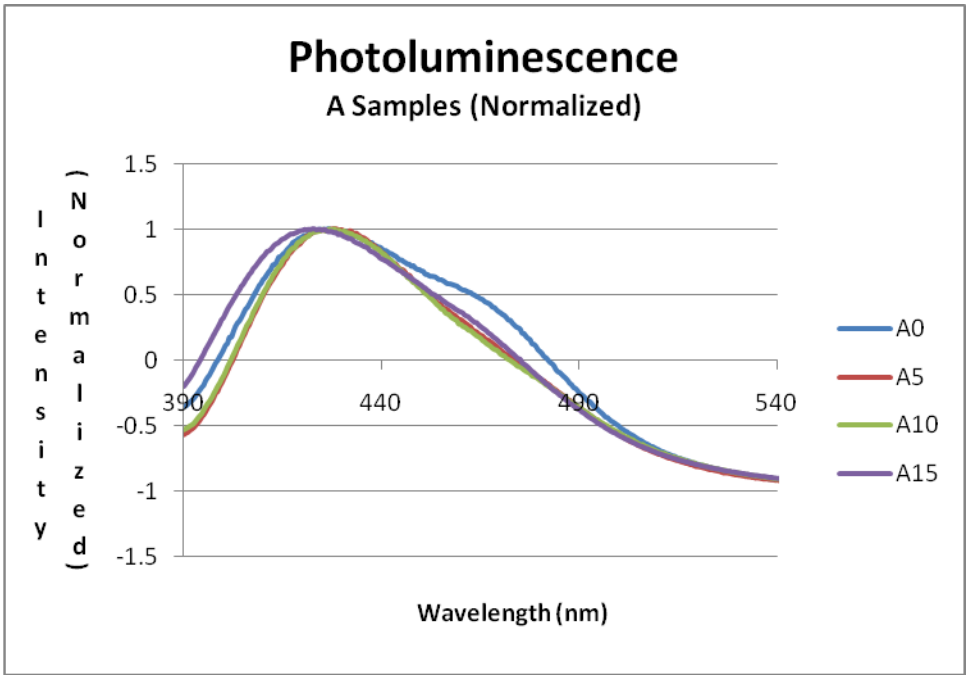

Figure 36. Photoluminescence DATA (Normalized) for Polymer A at 0%, 5%, 10% and 15% Weight Fractions of Nanoparticles (Samples; A5, A10 & A15)

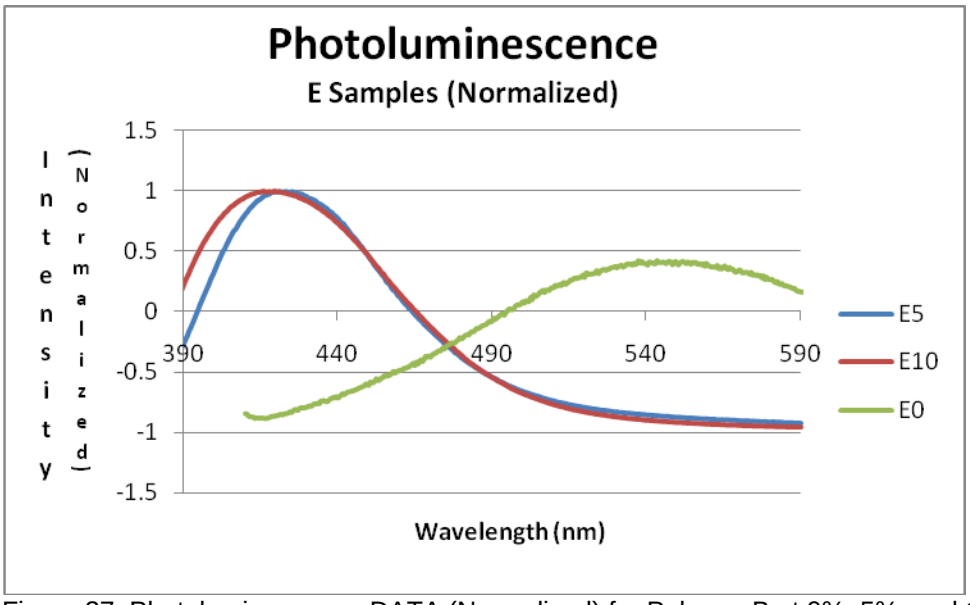

Figure 37. Photoluminescence DATA (Normalized) for Polymer B at 0%, 5%, and 10% Weight Fractions of Nanoparticles (Samples; E5 & E10)

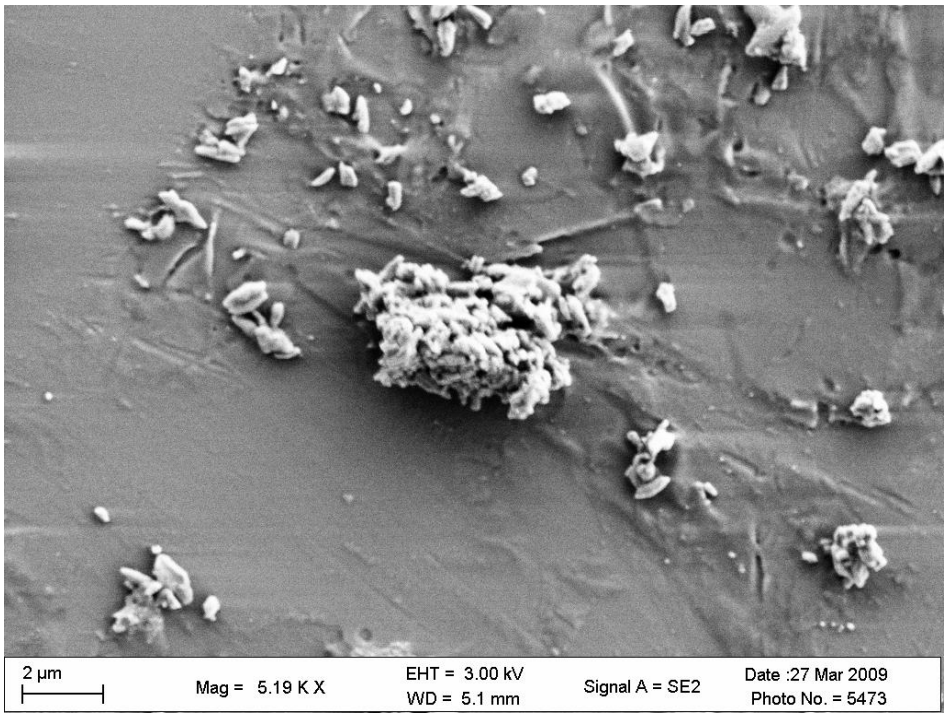

Figure 38. Polymer B with 10% Nanoparticles at 2 µm

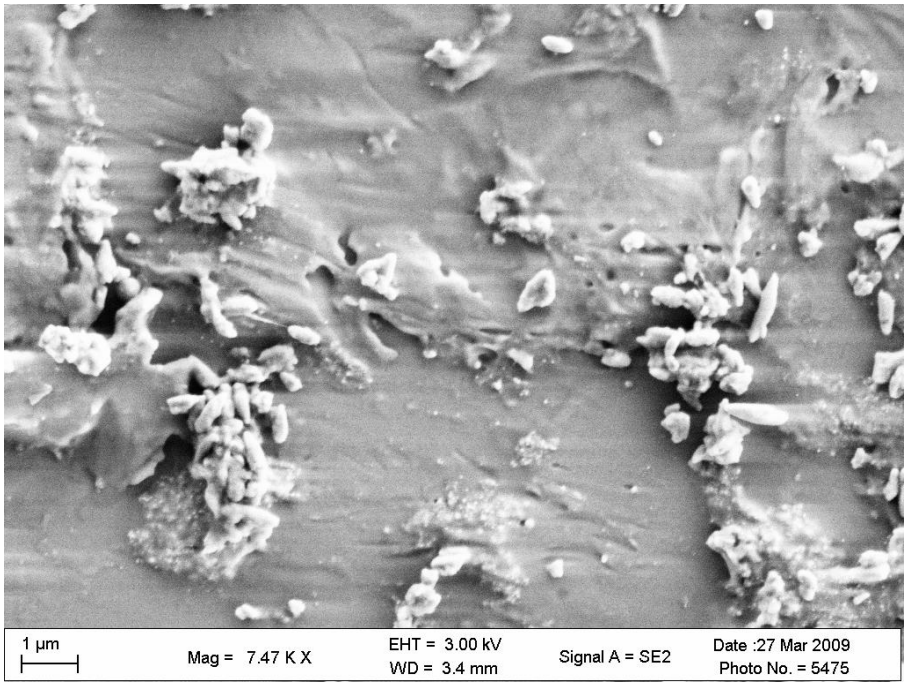

Figure 39. Polymer A with 10% Nanoparticles at 1 µm

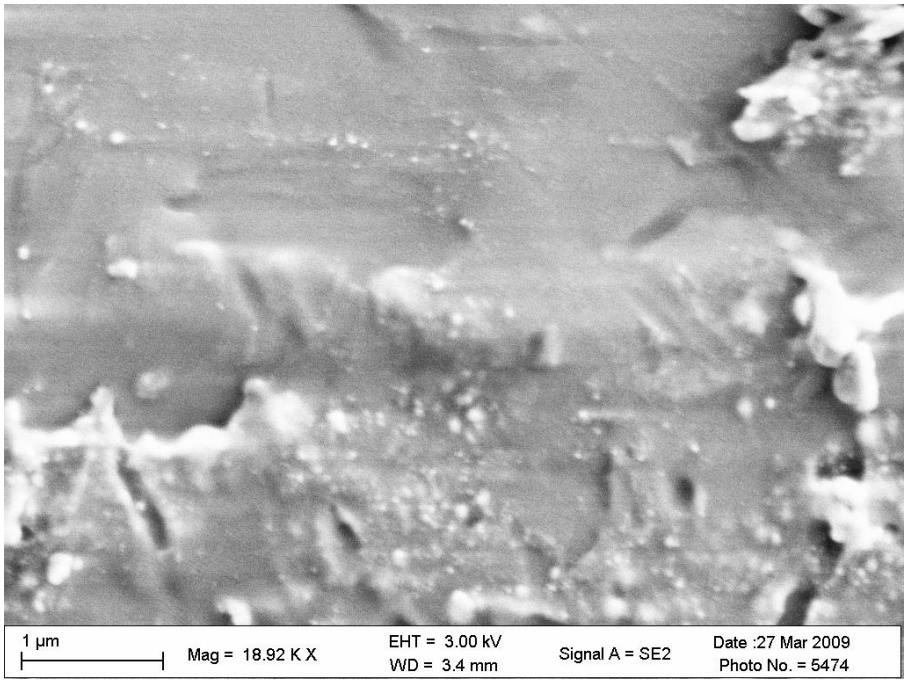

Figure 40. Polymer A with 10% Nanoparticles at 1 µm (Undulation)

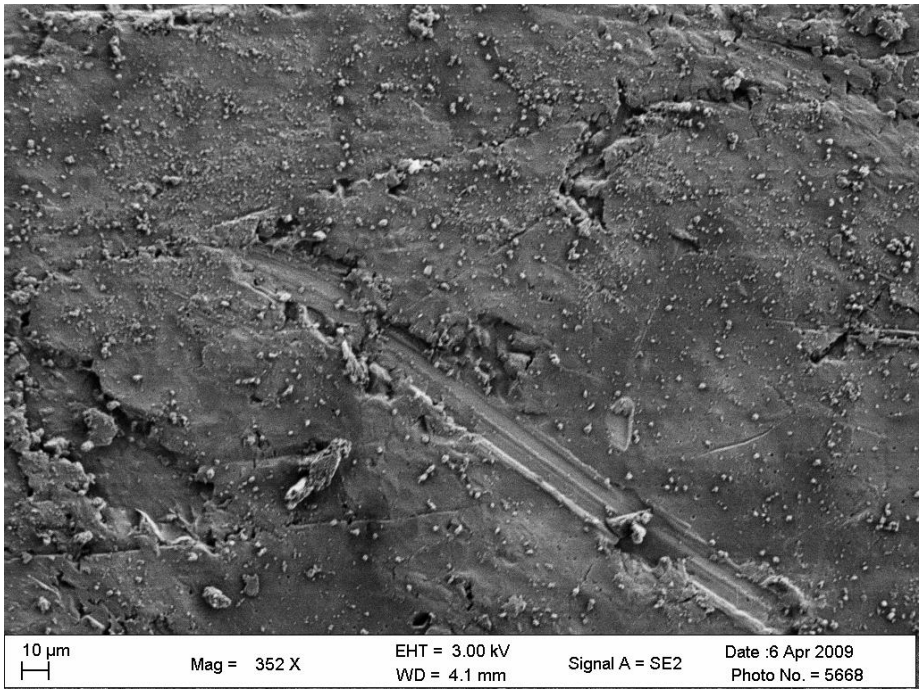

Figure 41. Polymer B with 10% Nanoparticles at 10 µm

TABLES

Table 1. Sample Preparation Method

Sample Preparation Method			
SAMPLE	**DESCRIPTION**	**ACTUAL % WEIGHT OF NANOPARTICLES**	**SPINCAST RPM X1000 & TIME (s)**
A0	Polymer A, emraldine salt 2.5% by weight	N/A	N/A
A5	A0+5% Wt Nanoparticles	5.15%	0.83 RPM 60 s
A10	A0+10% Wt Nanoparticles	10.97%	0.83 RPM 60 s
A15	A0+15% Wt Nanoparticles	15.66%	0.83 RPM 60 s
C0	Polymer B in Chloroform	N/A	N/A
C5	C0+5% Wt Nanoparticles	4.4%	0.90 RPM 60 s
C10	C0+10% Wt Nanoparticles	12.8%	0.90 RPM 60 s
C15	C0+15% Wt Nanoparticles	17.4	0.90 RPM 60 s
E0	C0+7 minute evaporation time before spin cast	N/A	N/A
E5	C0+5% Wt Nanoparticles	4.4%	0.60 RPM 2 s
E10	C0+10% Wt Nanoparticles	12.8%	0.60 RPM 2 s
E15	C0+15% Wt Nanoparticles	17.4	0.60 RPM 2 s

Table 2. Index of Refraction Standard Deviation

Index of Refraction Standard Deviation				
Sample	Standard Deviation		Sample	Standard Deviation
A0	0.10		**E0**	0.10
A5	0.05		**E5**	0.05
A10	0.02		**E10**	0.11
A15	0.03		**E15**	0.02

VITA

Matthew Fuller graduated with a BS in Aerospace Engineering from Mississippi State University in 1999. He went active duty Air Force as an engineer. He had several interesting engineering projects such as launching a DSP satellite, operationally testing Global Positioning System ground segment, teaching Air Force ROTC and cutting up and salvaging parts from an attrited C/KC-135 aircraft.